SYNTHESIS AND CHARACTERIZATION OF ELECTRON DEFICIENT HETEROCYCLES AS BUILDING BLOCKS FOR ELECTRONIC MATERIALS

Jihad Habeeb Saeed

Submitted in the Fulfilment of the Requirements for the Degree of Master in Science

September 2015

School of Chemistry

UNIVERSITY

of

GLASGOW

Abstract

This thesis describes the synthesis of a new electropolymerizable viologen derivative. A reasonably high-yielding route is reported, and a preliminary investigation of its polymerisation is described. The viologen and its precursors were examined by ^{1}H NMR, MS, IR and elemental analysis. The energies of the band gap for the materials have been calculated using UV-vis spectroscopy, and cyclic voltammetry was also used to estimate the oxidation and the reduction potentials and to calculate the HOMO and LUMO energies. Theoretical calculations were performed using DFT. The attempted synthesis of a new flavin-functionalised phenanthroline derivative is described. Unfortunately, the protocol used failed to provide the desired compounds.

Acknowledgments

Firstly, my uncountable praise to Al-Mighty Allah who guided me and gave me the strength to continue this learning process as it is only by His grace and the prayers of my loved ones that this momentous journey has reached its end.

I would like to show my gratitude to my academic supervisor, Prof. Graeme Cooke, for giving me the chance to work on this exciting project. His guidance, commitment and the dedication in the work in addition to his optimistic, motivation and his understanding shown in difficult times during the course of my time in his group have proved invaluable.

I also wish to thank Jim Tweedie for mass spectroscopic analysis. Special thanks to Dr. Stuart Caldwell and Dr Brian Fitzpatrick for all their help.

Also I would like to thank my fellow students for making the lab an enjoyable place to work.

Never could I have done alone without those people around me who have provided considerable support, my family and friends, especially my parents for their encouraging me.

Finally, I would like to thank my wife Nada children (Maab, Mustafa and Manaf), for all their help in terms of their own time dedicated to my support throughout my research.

Contents

Abbreviations

A.....Acceptor

BDTD .....Benzo[1,2-*b*:6,5-*b*′]dithiophene-4,5-dione

^{o}C.....Degrees Celsius

CV.....Cyclic Voltammetry

D.....Donor

DFT .....density functional theory

DMF.....Dimethylformamide

DMSO.....Dimethylsulphoxide

DNA.....Deoxyribonucleic acid

DSSC .....Dye sensitizer solar cells

e^{-}.....electrons

E.....Energy

$E_{1/2}$.....Half wave potential

EC.....Electrochromic

ET.....Electron transfer

eV.....Electron volt

Fc.....Ferrocene

FAD.....Flavinadeninedinucleotide

FMN.....Flavinmononucleotide

g.....Gram

HOMO.....Highest occupied molecular orbital

I.....Iodine

IR .....Infrared

ITO.....Indium tin oxide

L.....Litre

LUMO.....Lowest unoccupied molecular orbital

M.....Molar (Mol per litre)

Me.....Methyl

min.....Minute

mL.....Millilitre

MLCT.....Metal-to-ligandcharge transfer

mp.....Melting point

NAD.....Nicotinamide adenine dinucleotide

NDI..... Naphthalenediimide

Nm.....Nanometer

NMR.....Nuclear magnetic resonance

OFETs .....Organic field transistors

OLED .....Organic light-emitting diodes

ox.....Oxidation

OPVs .....Organic photovoltaics

PCBM .....Phenyl-C61-butyric acid methyl ester

Pd(C) .....Palladium (on carbon)

PEDOT:PSS ..... Poly(3,4-ethylenedioxythiophene) polystyrene sulfonate

Pt .....Platinum

PV ..... Photovoltaic solar cells

PVDF..... Polyvinylidene fluoride

red.....Reduction

Ru.....Ruthenium

S..... Ground state of photosensitizes

S*.....excited state of photosensitizes

S^{+}.....oxidation state of photosensitizes

SET ..... Single electron transfer

SnO_2.....Tin oxide

$TBAPF_6$.....Tetra-n-butyl ammonium hexafluorophosphate

TCO.....Transparent conducting oxides

TiO_2.....Titanium indium oxid

UV/Vis.....Ultraviolet/Visible light

Vs^{-1}.....Volts per second

λ.....Wavelength

Declaration:

I hereby declare that the substance of this thesis has not been submitted, nor is currently submitted in candidature for any other degree. Portions of the work described herein have been published elsewhere and are listed below.

I also declare that the work presented in this thesis is the result of my own investigations and where the work of other investigators has been used, this has been fully acknowledged within the text.

Jihad H. Saeed

1. Introduction

1.1 Electrically conducting polymers

Electrically conductive polymers (Figure 1) have realised a great deal of interest[1] in the area of electronic applications particularly in nonlinear optics, organic light-emitting diodes (OLED)[2], organic transistors, photovoltaic solar cells (PV)[3]. Conductive polymers can be presented as non-metallic semiconductors having electrical conductivity between a conductor and an insulator. The delocalized electronic structures of π-conjugated polymers tend to present quite rigid chains with modest flexibility and with reasonably strong inter chain attractive interactions.

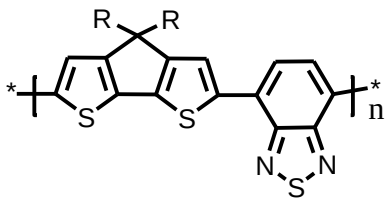

1

Figure 1. An electrically conducting polymer 1[4]

Conjugated polymers must have excellent electronic and mechanical properties to be useful in electronic applications. It is important to mention that such polymers should have sufficient solubility to guarantee solution processability and have high environmental stability. Also, these polymers should have suitable HOMO and LUMO energies, a low optical band gap to capture more solar energy and have a broad absorption spectrum. Furthermore, for accelerating charge transport, these conjugated polymers must have high hole mobility to reduce charge recombination and series resistance[4]. On the other hand, it has been found that the electrical conductivity can be affected by the molecular structures of the polymer depending on the degree of π-orbital overlap along the conjugated chain, the carrier mobility, and the energy gap[1]. Thus, most of these conducting polymers are synthesised *via* connecting electron-rich donor and electron-deficient acceptor segments along the conjugated polymer backbone, in either an alternating or a random fashion[5]. The electronic properties of the conductive polymers can also be altered in a controllable manner by adding a small amount of a well chosen impurity. This process is known as doping.

1.1.1 Chemical polymerisation.

Transition metal-catalyzed cross-coupling reactions can be considered as one of the most commonly used synthetic methodologies for the formation of new carbon-carbon bonds. Many organometallic reagents have been demonstrated to be used as nucleophiles for the cross-coupling reaction such as organolithiums[6] organostannanes[7,8] 1-alkenylcopper(1)[9] and organosilicon compounds[10]. Some of the organometallic reagents were used for C-C bond formations like Li (Murahashi)[11], B (Suzuki Miyaura)[12], Mg (Kumada-Corriu)[6], Al (Nozaki-Oshima, Negishi)[13], Si (Hiyama)[10], Cu (Normant)[9], Zn (Negishi)[14], Zr (Negishi)[15], and Sn (Stille)[16]. In addition, bonds such as C-H, C-C, C-N, C-O, C-P, and C-Metal plus heteroatom-H bond like N-H[17], O-H[18], P-H[19], and S-H[20] can also be obtained by Pd-catalyzed cross-coupling reactions.

The palladium-catalyzed cross-coupling reaction offers a general, powerful, valuable and versatile methodology for the creation of new carbon–carbon bonds. One reaction takes place between organoboron compounds and organic halides or triflates and has been called the Suzuki coupling[21]. It is known that the organoboron compounds are highly electrophilic although the organic groups on boron are so weakly nucleophilic that limits their use of reagents for ionic reactions. Therefore using negatively charged base will activate the boron atom and increase its nucleophilicity and so will permit it to transfer the organic group on boron to the adjacent positive center[22].

Stille and Suzuki reactions have been the most widely used aryl-aryl coupling reactions in the synthesis of conjugated polymers. The reaction between stannanes and halides to form C-C bonds is called Stille Coupling (Scheme 1). The main problem of this method is the toxicity of tin compounds.

$$R'\text{-}X + RSnBu_3 \xrightarrow{\text{Pd-catalyst}} R\text{-}R' + XSnBu_3$$

Scheme 1. Stille coupling

However, Suzuki coupling has the same versatility without the problem of using tin compounds (Scheme 2). It is a palladium-catalysed cross coupling between organoboronic acid and halides. Potassium trifluoroborates and organoboranes or boronate esters may be used instead of boronic acids.

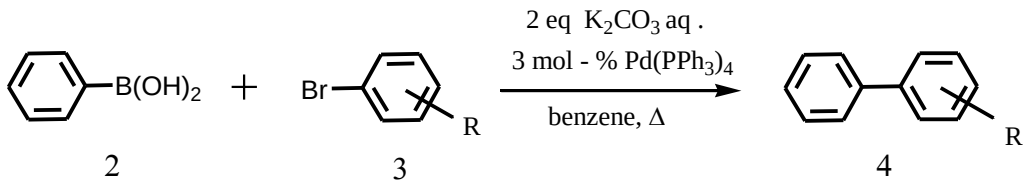

Scheme 2. Suzuki coupling

1.1.2 Electropolymerization.

The electropolymerization process can be simply defined as a polymerization under the influence of an electric current. The formation of electroactive polymers *via* reduction or oxidation of different organic compounds is called electropolymerization, which is a simple and reproducible way of forming organic or organometallic films on surfaces from monomers (Scheme 3). Electropolymerization is a very good way for developing modified electrodes for many reasons. Firstly, electropolymerization affords simplicity of targeting in the selective modification of multi electrode structures. In fact by applying the required current or potential, polymer formation can be targeted on the electrode of interest even by exposing the whole structure to the precursor solution. Secondly, compared to adsorbed and covalently linked modifiers like low-molecular- weight organic compounds or chemically synthesized polymers, the electropolymerization films are often more stable on electrode surfaces. Finally, the electropolymerization materials usually have some distinctive properties that do not exist in the corresponding monomers. These properties mainly concern electroactive polymers, which exhibit new sets of peaks in the cyclic voltammogram because of the appearance of new conjugated chains or modification of the existing ones in their structure. Electrochemistry has opened the way to facilitate handling polymer films. Additionally this cross-fertilization has enlarged and strengthened this field by opening of new applications like energy conversion and storage[23].

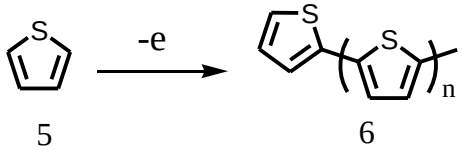

Scheme 3. Electropolymerization of thiophene.

1.2 Donor - acceptor alternative polymers.

Conjugated copolymers of alternating donor and acceptor units have attracted substantial interest as one of the most powerful strategies for band gap engineering in π-conjugated polymers[24]. Alternating donors and acceptors in copolymers results in small HOMO–LUMO gaps, leading to absorption spectra extending into the near-infrared region[25]. For instance poly(terthiophene) has been linked with C_{60}-pyrrolidine **7** in alternating donor-acceptor systems (Figure 2-a)[26]. It has also been found that an interesting tunable optical characteristics can be achieved by attaching thiophene substituents as electron donor with phenazine as electron acceptor units **8** (Figure 2-b)[27].

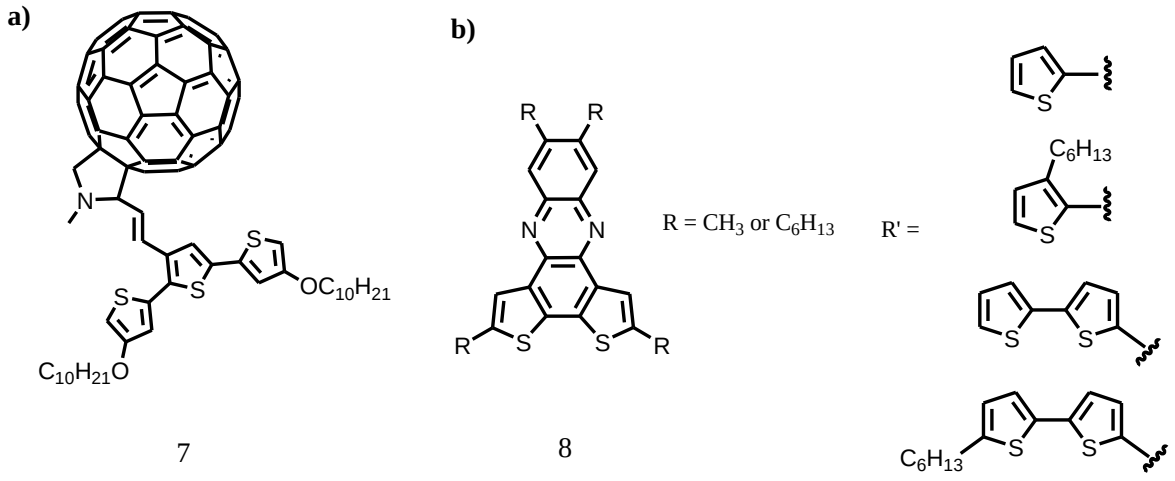

7 8

Figure 2. Alternating donors and acceptor copolymers[22,23]

However, for further improving of the physical and electronic properties, benzo[1,2-*b*:6,5-*b*′]dithiophene-4,5-dione (BDTD) has been used to develop π-conjugated polymers as they provide access to various acceptor and donor molecules by converting the ketone groups in the diones into other organic functionalities (Figure 3)[28]. These donor-acceptor polyaromatic compounds have received considerable attention as π–π stacking and the thienyl S....S contacts contribute to the intermolecular charge transport in the solid state[29].

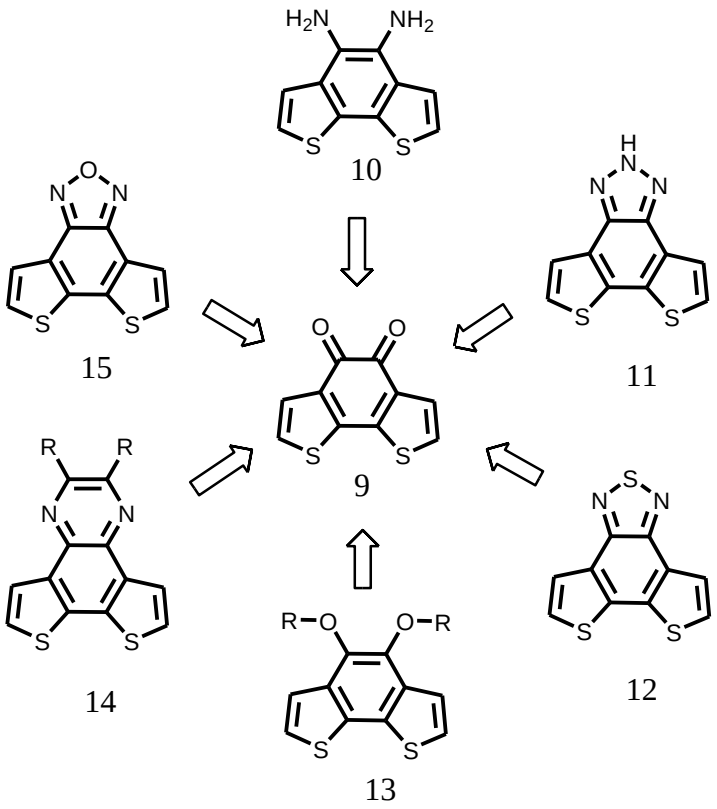

Figure 3. Benzo[1,2-b:6,5-b′]dithiophene-4,5-dione (BDTD) and its chemical transformations[28]

As a convenient approach to tune the optoelectronic properties of donor–acceptor (D – A) polymers, thiophene supplemented fused-aromatic thienopyrazine systems (Figure 4-a) have been employed to produce low band gap polymers when copolymerized with fluorene and cyclopentadithiophene. The improved face to face π–π stacking afforded by the fused thienopyrazine units results in high charge carrier mobility in thin film transistor devices and moderate power conversion efficiencies in bulk heterojunction solar cell devices[30]. In addition, narrow band gap D – A conjugated polymers based on quinoxaline monomers as acceptors (Figure 4-b) show red-shifted absorption spectra due to the enlarged planar polycyclic aromatic rings. The copolymers' mobilities are also considerably increased because of the reduced steric hindrance and enlarged fused structural planarity. Although bulk heterojunction polymer solar cells based on blends of the copolymers with a fullerene derivative as acceptor achieved power conversion efficiency up to 7.4% , but the studies that followed reported values up to > 10%[31].

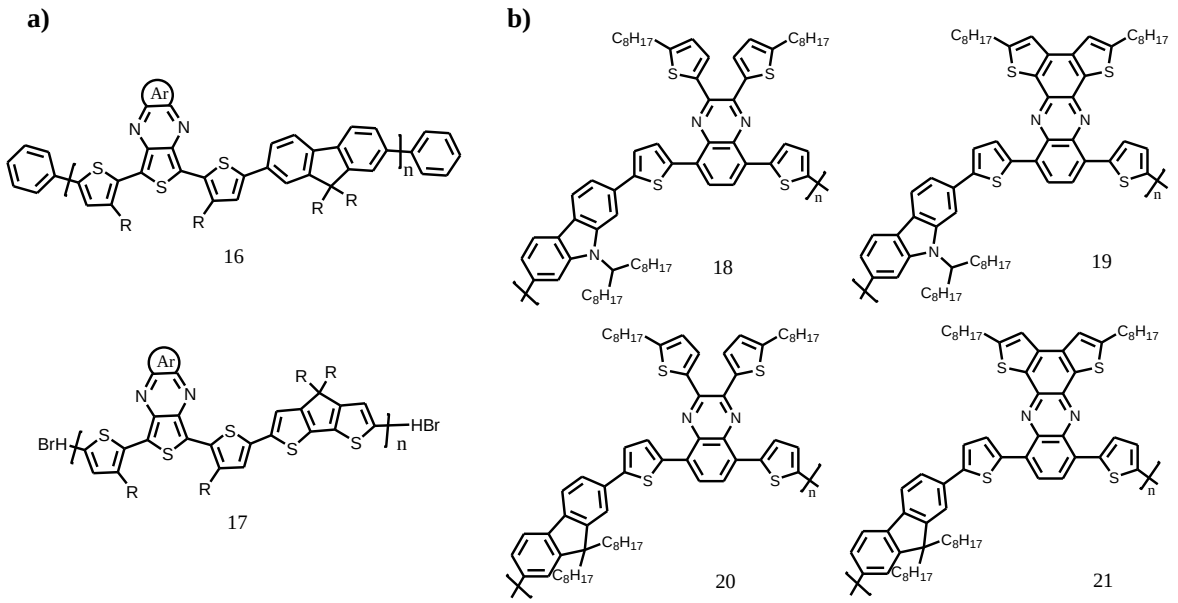

Figure 4. Donor-acceptor (D-A) conjugated polymers based on, a) thiophene supplemented fused-aromatic thienopyrazine system[30]. b) thiophene substituted quinoxaline monomer as acceptors[31]

Consequently, D – A copolymers have received considerable attention for their relatively high electrical conductivity[32] and small band gaps[33]. Thus, alternating donor-acceptor repeat units in thiophene-based polymers prepared by modified Stille polymerizations exhibit a significant decrease in the band gap by means of the intramolecular charge transfer[34]. In fact, in heterocyclic chemistry, it is recognized that the five-membered ring heterocycles like thiophene and furan have a π-excessive nature while six-membered ring compounds such as electron-withdrawing imine (C=N) nitrogens like pyridine and quinoxaline have a π-deficient nature[35]. Therefore, in general it has been shown that the linear combination of π-conjugated heterocycles of this type leads to polymers possessing charge transfer structures which show interesting and unique chemical and physical properties[36].

1.3 Dye-sensitized solar cells DSSC

One of the most serious problems facing the world today is that concerning the availability and distribution of energy and the search of alternative energy sources is a global priority. Solar energy is the best choice since the solar energy is clean, abundant, renewable and reliable in most regions of the earth. Although bulk heterojunction solar cells formed from electron rich polymers and accepter units such as phenyl-C61-butyric acid methyl ester

(PCBM) have given rise to competitive power conversion efficiencies, other technologies are becoming important too[37]. For example, dye-sensitized solar cells (DSSC)[38] can be considered as low-cost solar cells that belongs to the group of thin film solar cells[39]. Michael Grätzel in 1988 with Brian O'Regan developed the first high efficiency DSSC in 1991[40].

Although DSSCs have a number of attractive characteristics like they can be simply fabricated by using roll-printing techniques, they are semi-flexible and semi-transparent plus most of the materials used are low-cost, their conversion efficiency is not yet at the required level. When for widespread use solar cells are placed in the sun (Figure 5), photons of the sunlight can excite electrons on the p-type side (or the donor) of the cell by a process called photoexcitation. In some materials, sunlight can provide energy equal to or higher than that of the band gap which requires pushing an electron out of the lower-energy valence band into the higher-energy conduction band. Electrical current can be created when a load is placed across the cell as a whole, so electrons can flow out of the p-type side into the n-type side (or the acceptor), losing energy while moving through the external circuit, to flow back into the p-type material (or the donor) where they can re-combine with the valence-band hole[41].

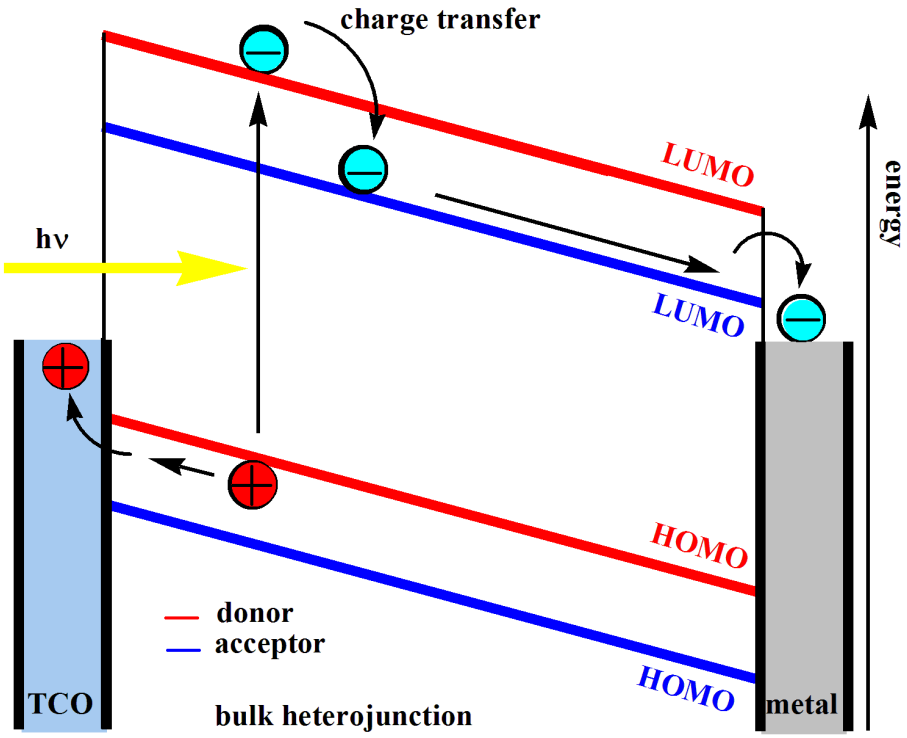

Figure 5. Energy levels of organic bulk heterojunction solar cells

Modern DSSCs (Figure 6) are composed of two electrodes immersed in an electrolyte solution which is usually a mixture of a photosensitive ruthenium-polypyridine dye and a solvent. The two electrodes are joined and sealed together to prevent the electrolyte from leaking. The anode is made of fluoride-doped tin dioxide (SnO_2:F) deposited on the back of a glass plate. A highly porous layer with a very high surface area of titanium dioxide (TiO_2) nanoparticles is deposited on the back of this conductive layer. When soaking the film in the dye solution, a thin layer of the dye is appeared covalently bonded to the surface of the TiO_2. The cathode is made of a thin layer of the iodide electrolyte spread over a conductive sheet of platinum. When sunlight passes through the transparent layer into the sensitized dye, the excited dye injects an electron into the TiO_2 to flow toward the external circuit, then to be re-introduced into the cell on a platinum electrode on the back. The electrolyte then transports the electrons back to the dye molecules. It is important to mention that the TiO_2 is used just for charge transport and the photoelectrons are provided from a separate photosensitive dye while the charge separation takes place at the surfaces between the dye - semiconductor and the electrolyte[42].

The incident photon enters the cell through the transparent SnO_2:F, and is absorbed by Ru complex photosensitizers that are adsorbed on the TiO_2 surface. Photons from sun light

should strike the photosensitizers with enough energy to excite electrons from the ground state (S) to the excited state (S*).

$$S + h\nu \rightarrow S^*$$

Electrons can then be injected directly into the conduction band of the TiO_2 by the oxidation of the photosensitizer (S*) to (S^+).

$$S^* \rightarrow S^+ + e^- (TiO_2)$$

The injected electron in the conduction band of TiO_2 moves by diffusion toward the transparent conducting oxide and then through the circuit, to the counter electrode.

The oxidized photosensitizer (S^+) accepts electrons, in order not to be decomposed, from the iodide ion I^- the redox mediator which leads to regeneration of the ground state (S) and the iodide I^- electrolyte is oxidized to the oxidized state triiodide I_3^-.

$$S^+ + e^- \rightarrow S$$

The triiodide I_3^- then recovers its missing electron by mechanically diffusing toward the counter electrode, and then it is reduced to I^- ions[43].

$$I_3^- + 2\ e^- \rightarrow 3\ I^-$$

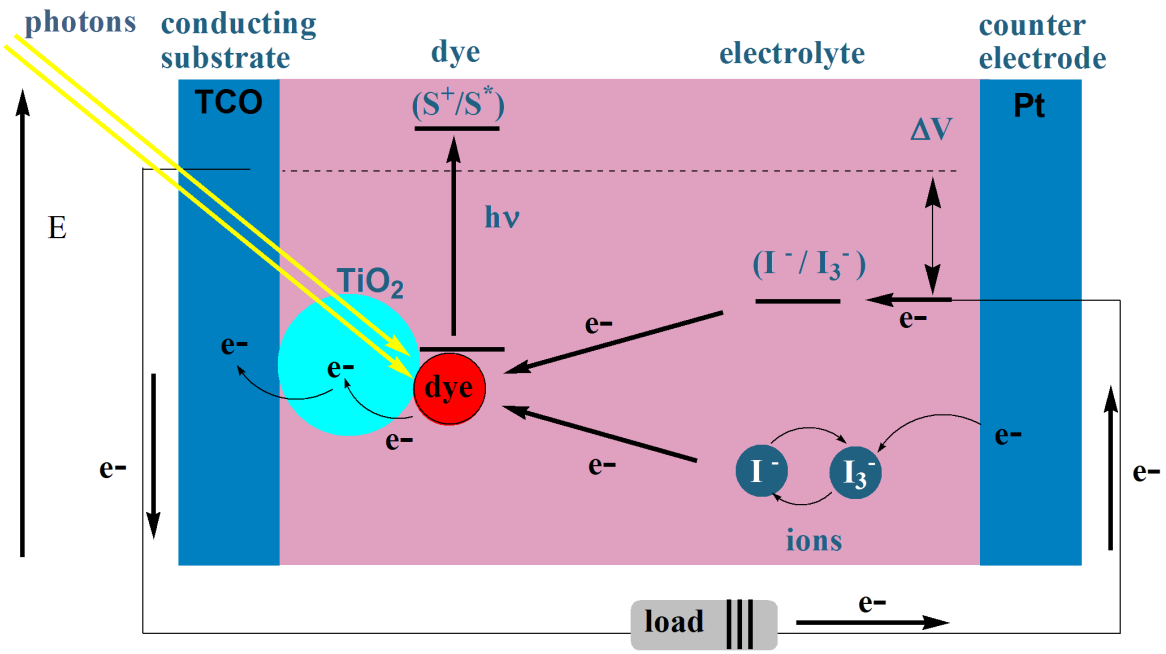

Figure 6. Schematic representation of the principle of the dye-sensitized photovoltaic cell indicating the electron energy level is the difference, ΔV, between the quasi-Fermi level of TiO_2 under illumination and the electrochemical potential of the electrolyte. The latter is equal to the potential of the redox couple (I^-/I_3^-) used to mediate charge transfer between the electrodes. S, sensitizer; S*, electronically exited sensitizer; S^+, oxidized sensitizer[40].

DSSCs are considered as a promising solution for exploiting the energy of the sun and converting it into electrical energy with power conversion efficiencies now exceeding the value of 12%, using a donor-π-acceptor zinc porphyrin dye as sensitizer with a Co(II/III)tris(bipyridyl)–based redox electrolyte (Figure 7). High photovoltages have been obtained from the compound **22** which significantly hinders the rate of interfacial back electron transfer from the conduction band of the nanocrystalline TiO_2 film to the oxidized cobalt mediator. In addition, large photocurrents were generated because it harvests sunlight across the visible spectrum[44].

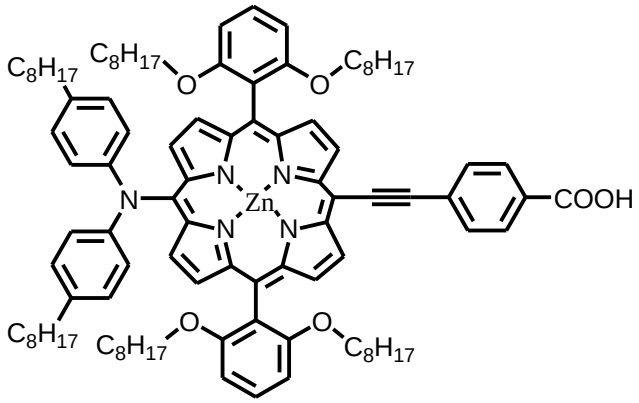

22

Figure 7. The molecular structures of the porphyrin dye 22[44].

As this thesis aims to develop new conducting polymers featuring viologen units and new flavin and phenanthroline incorporating dyes for DSSCs a brief summary of their properties and applications will now be described.

1.4 Examples of accepters and their incorporation into polymers and Dye-sensitized solar cells (DSSCs).

1.4.1 Viologens

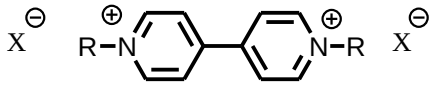

23

Figure 8. Viologen (4,4'-bipyridyl salt).

Viologens are bipyridinium derivatives of 4,4'-bipyridyl[45] (Figure 8). This group of compounds can be synthesized by the reaction of bipyridyl **24** with alkyl halide to yield the dication **23** (viologen). Viologens are electron deficient and form a coloured charge-transfer complexes[45] with many electron-rich donor species. Consequently viologens can be reduced easily to the radical mono cation[45], which is colored blue[46]. The further reduction of the radical mono cation produces a yellow quinoid (Scheme 4). The ability of viologens to change color reversibly due to the electrochemical redox reactions made them appropriate to be used for electrochromic systems.

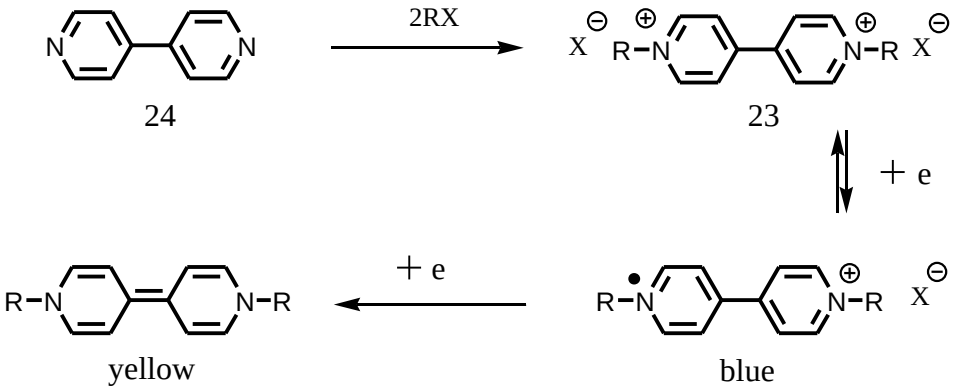

Scheme 4. The redox chemistry of viologen

The extended viologens in which two pyridylium rings are connected by a π-conjugated fragment such as phenylene [47,48,49], thiophene [47,50,51] furan[47], and polyene[52,] can be reduced to the "neutral" viologen (Figure 9). The hybrid structure of the neutral form results from the resonance structure of the quinoid and the biradical. The driving force for the biradical is the restoration of aromaticity due to the formation of a biphenyl unit.

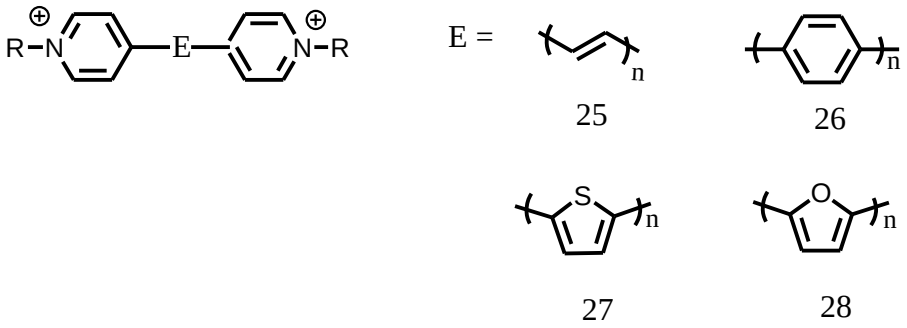

Figure 9. Examples of extended viologens [46].

Extended "neutral" viologens have been considered as strong electron donors because when a standard viologen in its neutral form gives up two electrons to form a dication, the two quinoid rings are converted to aromatic rings, providing the driving force for the reaction and making it a stronger electron donor than a standard neutral viologen[46]. However, studies showed that the diradical represent two different spin states of the molecule: a singlet diradical or a triplet diradical. The singlet and triplet diradical would exist as a resonance structure with the quinoid form (Figure 10)[46].

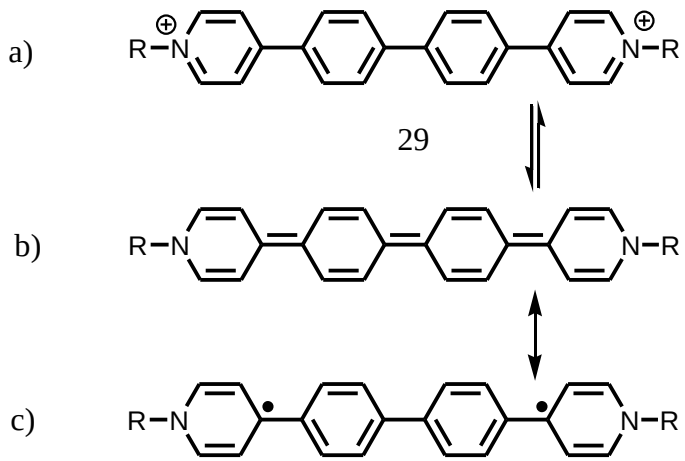

Figure 10. a) The dication of the extended viologen. b) Quinoid form of c) Diradical (singlet or triplet) form[46].

The "flexible" 2,2-bipyridine and the "rigid" 1,10-phenanthroline viologens where the two nitrogen atoms are connected by a chain have been studied as electron acceptors[53]. A single electron transfer (SET) easily takes place from the donor molecule to the viologen acceptor, giving the radical cation $\mathbf{A}^{\bullet+}$. 2,2-Bipyridine forms a twisted geometry upon reduction giving rise to a coplanar shape. Meanwhile, 1,10-phenanthroline **B** form undergoes no such structural change upon reduction due to the fused ring system, as illustrated in Scheme 5. In addition, it has been shown that the SET to 1,10-phenanthroline is 10^5–10^6 times faster than the SET to 2,2-bipyridine. Consequently, The difference in the reorganization energy is attributable to the difference in the structural change of the viologen accompanying the SET[53].

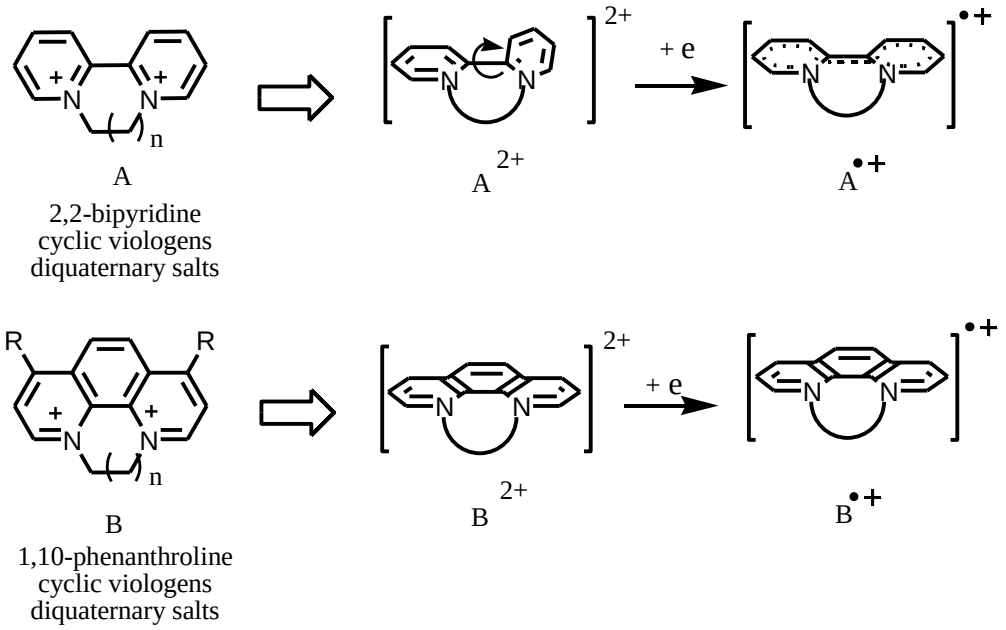

Scheme 5. The electronic structure of 2,2-bipyridine and 1,10-phenanthroline cyclic viologens upon single electron transfer (SET) [53]

The viologen based π-conjugated polymer, poly-[*N*,*N*-(1,4-divinylbenzene-*β*,*β*′-diyl)-4,4′-bipyridinium dibromide], was studied and showed properties of conductivity and electroactivity (Figure 11)[54].

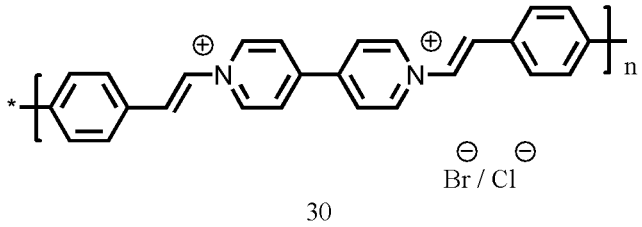

Figure 11. poly-[*N*,*N*-(1,4-divinylbenzene-*β*,*β*′-diyl)-4,4′-bipyridinium dibromide][49]

In addition, electrochromic systems of low molecular mass viologens **31** have been incorporated into a polymer matrix **32** without any phase separation due to the presence of hydrogen and ionic bonds (Figure 12)[55].

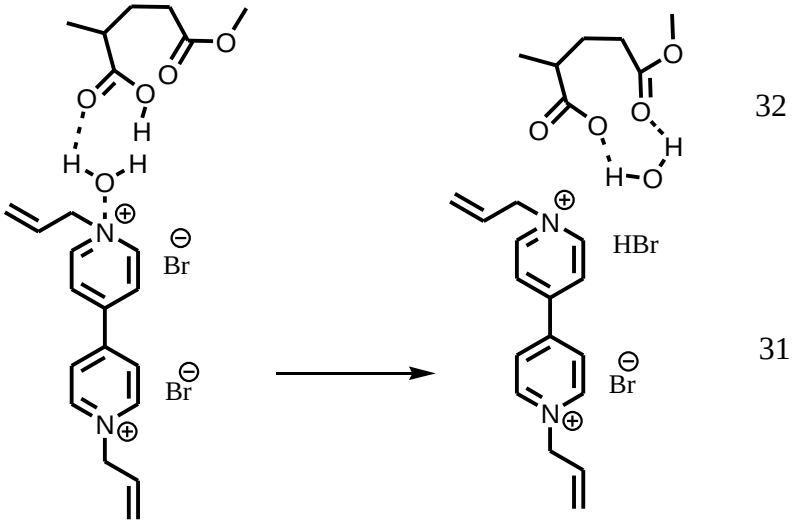

Figure 12. Electrochromic systems based on noncovalently associated polymer–viologen complexes[55].

Polymers functionalized with viologen as side chains have also fascinated researchers to their possible applications in redox or electrocatalysis[56], microelectrochemical devices[57], sensors[58], and electrochromic devices[59]. The characterization of polythiophenes functionalized with viologen **33** (Figure 13), revealed that the properties can be influenced and tuned by the proper choice of the parent thiophene unit[60].

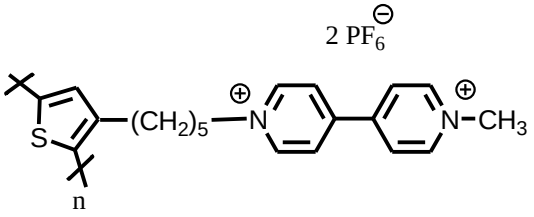

33

Figure 13. Viologen functionalized polythiophene[60-61]

Viologen moieties have been covalently linked to the polymeric chain either as side groups[62] and pendant[63] or as interconnecting units[64]. In viologen functionalized polythiophenes, the polythiophene chain represent the electrically conducting backbone to which the redox active viologen moieties can be covalently linked by alkyl chains of varying lengths[61]. Effects of the viologen on the electronic properties of the polythiophene backbone in its conducting state have been studied. Wudl revealed a localization of the charge carriers in polymer **34** (Figure 14)[65].

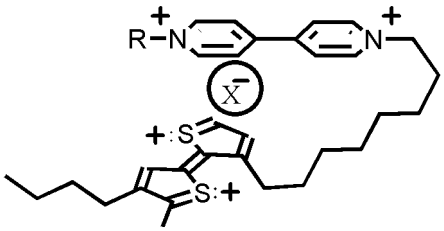

34

Figure 14. Viologen functionalized polylthiophenes[65].

The diquaternary salt of phenathroline **35** (Figure 15) has been proven to be a useful building block in supramolecular chemistry, benefiting from its features of rigidity, planarity, aromaticity and the π-electron-deficient character and extended π-surface to ensure efficient supramolecular associations with various π-electron-rich counterparts such as compounds **36-38**[66].

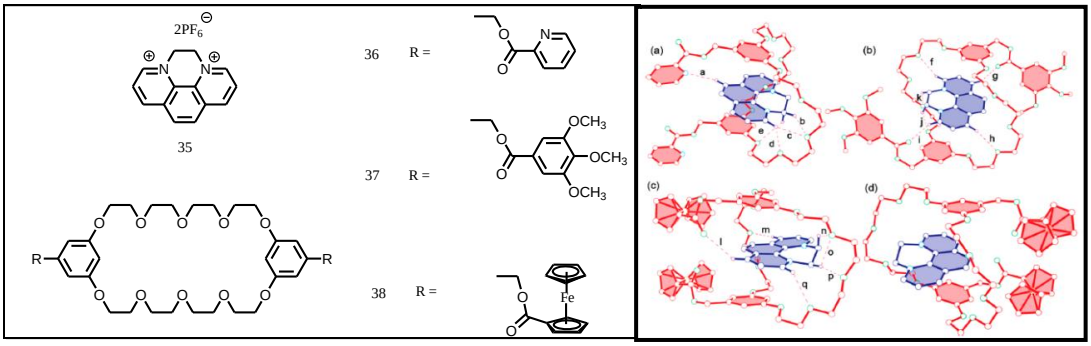

Figure 15. The diquaternary salt of phenathroline as building block in supramolecular chemistry and the X-ray structures of Host (red) - guest (blue) system[66].

Viologen-like monomers which have electron-deficient pyridinium rings that present low LUMO energies and a planar structure for extended *π*-electron delocalization have been polymerized to produce the water soluble n-type poly (pyridinium phenylenes, **39-41**) (Figure 16). These conjugated polymers have reversible redox behaviour, good electron affinities, and high electrical conductivity that make them attractive for the production of photovoltaic cells, light emitting diodes, and field-effect transistors[67]

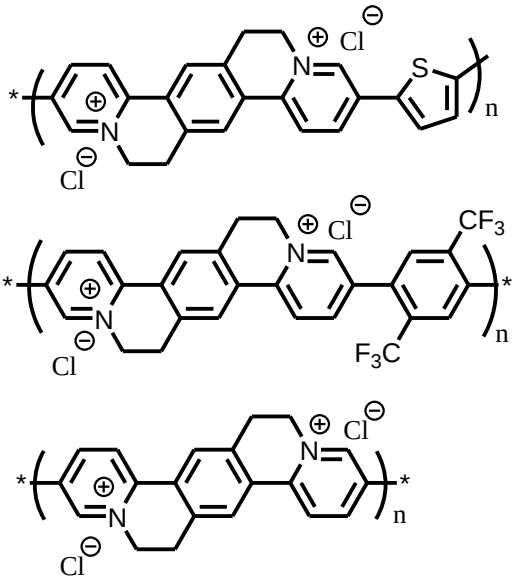

Figure 16. Water-soluble n-type poly(pyridinium phenylenes)[67]

Naphthyl-functionalized viologens (MV^{2+}) were introduced as quenchers in a series of nonaggregating carboxylate-functionalized poly(phenylene ethynylene)s (PPEs) that adsorbed onto Eu^{3+}-polystyrene particles to study the influence of electrostatic and hydrophobic interactions and for measuring the fluorescence quenching of films in an aqueous environment (Figure 17)[68].

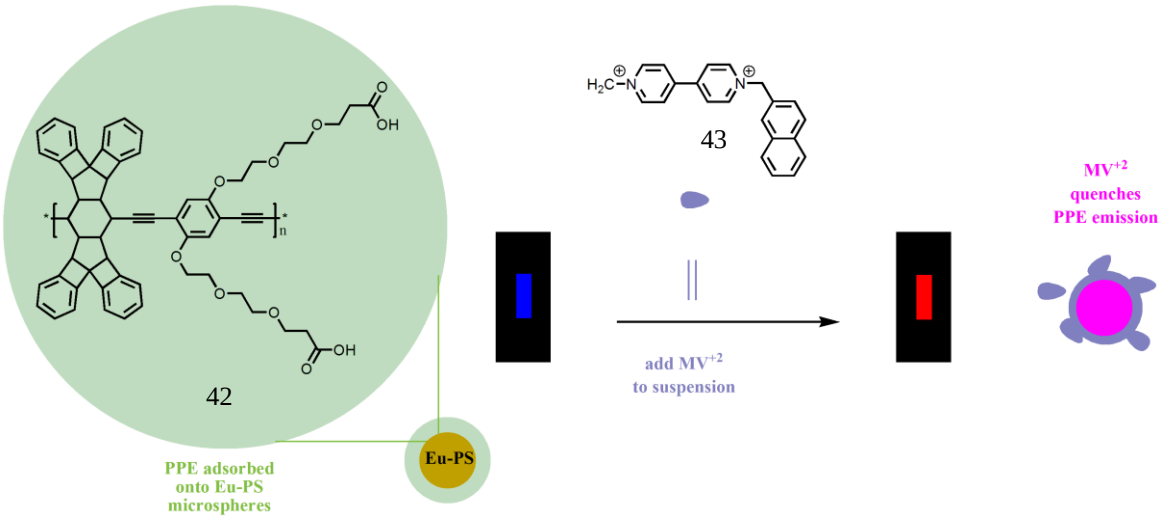

Figure 17. Series of nonaggregating carboxylate-functionalized poly(phenylene ethynylene)s (PPEs) adsorbed onto Eu^{3+}-polystyrene particles quenched by naphthyl-functionalized viologens (MV^{2+})[68].

Viologens have been employed in DSSCs extensively. For example a viologen polymer was used as a charge-storable electrode and an aqueous electrolyte in DSSC[69]. In addition, DSSCs fabricated using viologen impregnated polyvinylidene fluoride (PVDF) are very encouraging in terms of their photovoltaic performance[70]. Also, a dual function device comprising of a DSSC and electrochromic (EC) display was fabricated using two dyes, an electrochromic dye of a modified viologen for colouring and a sensitizer of ruthenium dye for light-harvesting. In this device the electrochromic dye was co-absorbed with the sensitizer dye onto a single nanocrystalline film. This device worked in such way that two opposite electron transfer processes take place in the same film (electrode). An energy power conversion efficiency 1.1% was achieved (Figure 18)[71].

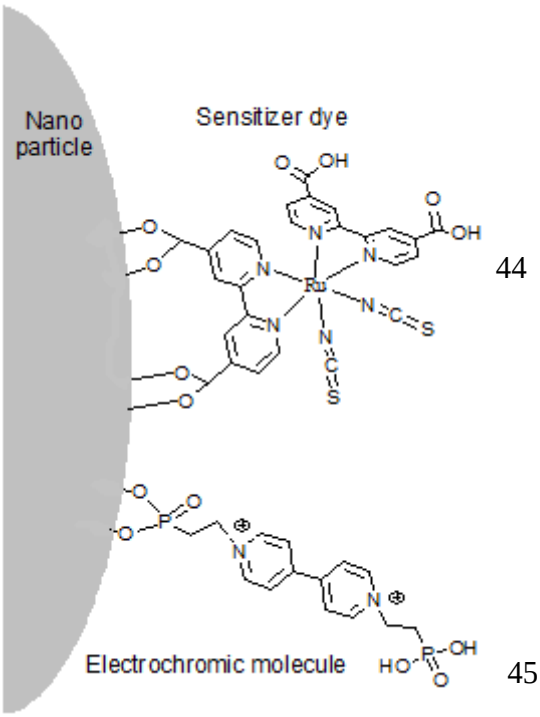

Figure 18. A TiO_2 layer as a dual function solar cell containing ruthenium and viologen dye[71].

1.4.2 Phenanthrolines

The 1,10-phenanthroline unit is rigid, and affords two nitrogen atoms whose free electron pairs are well located to act cooperatively in binding transition metal cations. The unit has been widely used as a ligand in metal complexes. Moreover the metal-phenanthroline complexes have been used in DSSCs because of their unique combination of chemical stability, redox properties, photophysical properties and excited state lifetime[72].

Phenanthrolines have been used, due to their interesting luminescence properties, in many applications. For instance, incorporating phenanthroline derivative possessing hydrogen bonding-donating abilities with low-dimensional inorganic networks helped to achieve reduced band gap materials[73]. Additionally, the chemistry of phenanthroline complexes has been studied intensively, for example, complex **46** is non-phosphorescent due to a strong intermolecular charge-transfer. However upon exposure to thiols, metal-ligand charge transfer is switched on resulting in phosphorescence (Figure 19)[74].

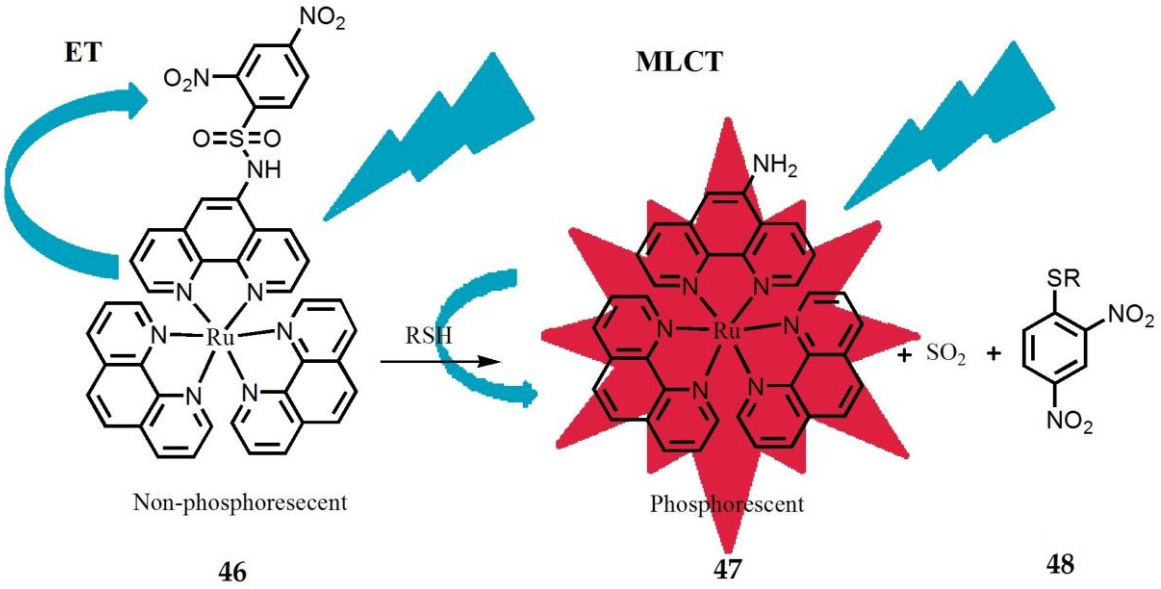

Figure 19. An OFF-ON red-emitting phosphorescent thiol probe[74]

Photo-physical spectroscopy studies revealed that the photovoltaic performance of phenanthroline-based ruthenium complexes for DSSC devices is rather sensitive to the substituents on the ancillary ligands. It has been shown the power conversion enhancement for the fluoro-substituted system is 24% and 66% higher than those of *N,N*-

dimethyl-substituted and methyl-substituted respectively. As fluoro-substituted complex increases the dye's density on TiO_2, the dye tunes the localization of the boundary orbitals appropriately, and enhances the electron lifetime for TiO_2 films (Figure 20)[75].

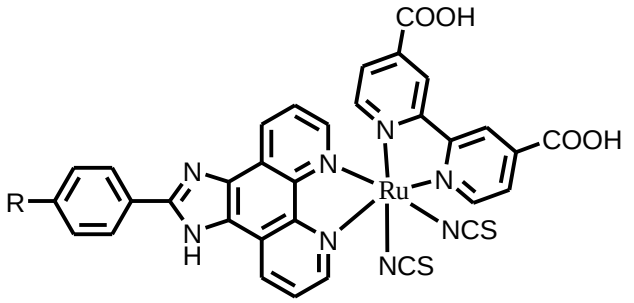

Figure 20. Molecular structure of the dyes[75].

Furthermore, phenenthroline complexes **52** have been extensively investigated as efficient light-harvesting molecules when adsorbed onto the surface of semiconductor thin films utilized as working electrodes on DSSCs[76]. Additionally, water soluble ruthenium phenanthroline complex **53** offered an advantage to construct DSSCs from aqueous solution. The cell was fabricated using a PEDOT:PSS counter electrode. The power conversion efficiency was encouraging for DSSCs utilizing a PEDOT:PSS counter electrode[77] (Figure 21).

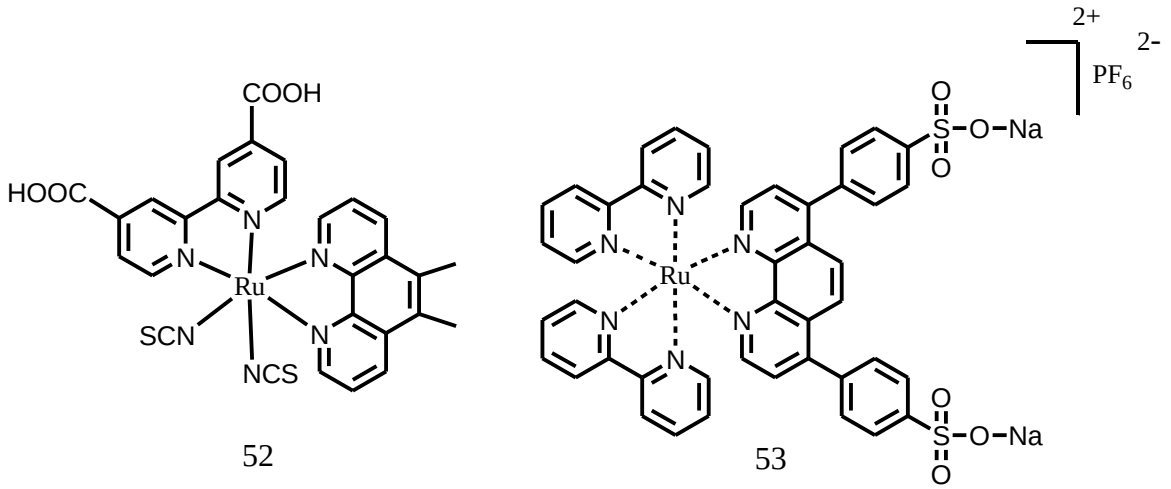

Figure 21. Phenanthroline-ruthenium complexes[76],[77].

1.4.3 Flavins

The word flavin **54** refers to the 10-substituted 7,8-dimethyl-2,3,4,10-tetrahydro-benzo[*g*]pteridine-2,4-diones, lumiflavin (7,8,10-trimethyl-10*H*-benzo[*g*]pteridine-2,4-dione) being the basic molecule of all other derivatives, *e.g.*, vitamin B_2 (riboflavin), flavin mononucleotide (FMN) and flavin adenine dinucleotide (FAD)[78]. Furthermore, flavins are group of compounds containing isoalloxazines that represent two classes of nitrogen heterocycles with active centers at N(1), N(3), N(5) and N(10), and at both carbonyl oxygens at C(2) and C(4) (Figure 22)[79].

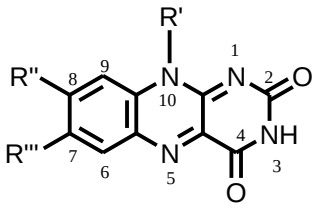

54

Figure 22. Flavins.

Many spectroscopic and photophysical studies have been performed on flavins[78]. The reason behind the large number of studies comes from the understanding of flavins biological importance and their attractive photophysical and photochemical features[80]. The photochemistry of flavins and the photophysical properties of alloxazines and isoalloxazines have been studied and have received attention from different points of views[81]. Accordingly the effects of the photoreduction and the photochemical addition reactions of flavins have been investigated in order to discuss the nature of the excited states involved in product formation[82]. The lowest excited singlet and triplet states of flavins have been studied via luminescence polarization. The study indicated that the fluorescent and phosphorescent states of flavins show **(π - π*)** transitions. On the other hand, the (n, π*) states play an important role in the luminescence processes of flavins, particularly of alloxazines. It has also been shown that in polar solvent at room temperature, the fluorescence quantum yield of some flavins is quite low and intersystem crossing is very efficient[83].

Hydrogen bonds occupy a vital role in the flavin's photophysics and photochemistry both in solutions and in the solid state. It has been found that flavin can form hydrogen-bonded complexes with a variety of molecules, such as acetic acid or methanol and the photoexcitation of some hydrogen-bonded complexes, as in the case of acetic acid, may cause excited-state proton transfer. Theoretical calculations similar to those observed experimentally, confirmed the role of the hydrogen-bonded complexes, forming stable eight membered cyclic configurations of such complexes (Figure 23)[84,85].

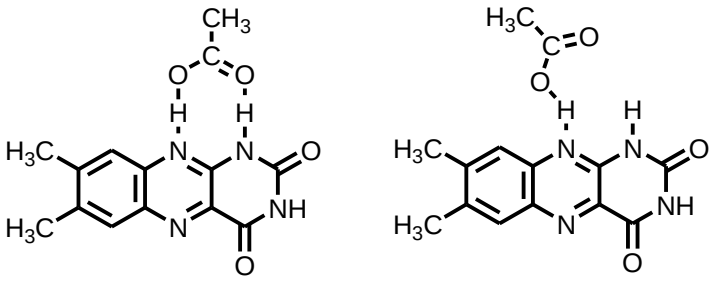

A 55 B

Figure 23. (A) Structure of eight membered cyclic complexes between flavin and acetic acid, (B) Structure of an open complex between two molecules.

Pterins and flavins have been described as excellent ligands for coordination to metals at the O(4)–N(5) chelating sites (Figure 24)[86]. Recently iridium(III) complex has been fabricated with flavin and has revealed a reversible redox processes (Figure 25)[87].

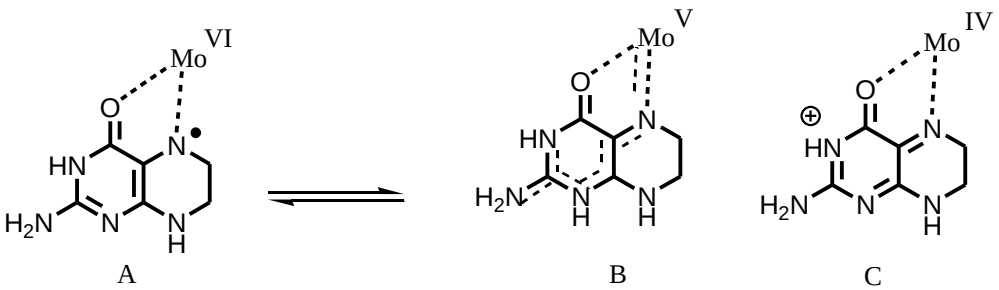

A B C

56

Figure 24. Pterins acting as important ligands[86].

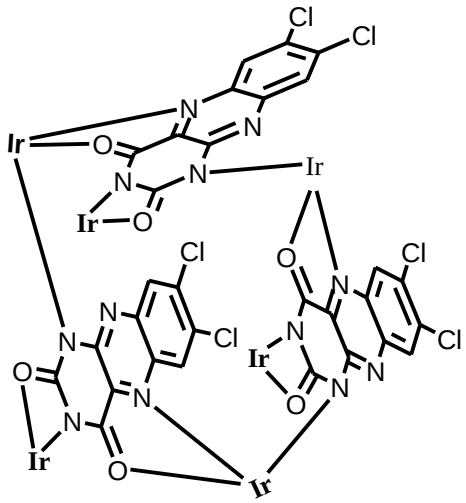

57

Figure 25. Iridium(III) complex[87]

1.4.3.1 Flavoenzymes

Flavoenzymes are an interesting class of proteins that catalyze a range of redox transformations in biological systems. Riboflavin, (vitamin B_2)**,** is a yellow heterocyclic isoalloxazine chromophore (Figure 26) which is the central component of the two active redox cofactors FAD (flavin adenine dinucleotide) and FMN (flavin mononucleotide) and it is essential for a range of flavoprotein enzyme reactions[88]. These reactions vary from oxidations and dehydrogenations to hydroxylations and electron transfer processes. Flavoenzymes and flavin analogues have rich photochemistry and photobiology because the isoalloxazine ring system allows them to contribute in various catalytic reactions and the photoexcitation of the ground state leading to different redox activities. Flavins, 7,8–dimethylisoalloxazine[89], or to be more systematic, 7,8–dimethylbenzo [g] pteridine – 2,4(3H, 10H)–dione are versatile catalysts, as displayed by two associated properties. Firstly, flavins can undergo both two-electron and one-electron chemistry. Firstly they can act as redox switches between two-electron donors (e.g., oxidation of NADH to NAD) and one-electron acceptors. Secondly, they can work as a cofactor for both two electrons reductions and four-electron reductive activation and cleavage in monooxygenation reactions[90]**.**

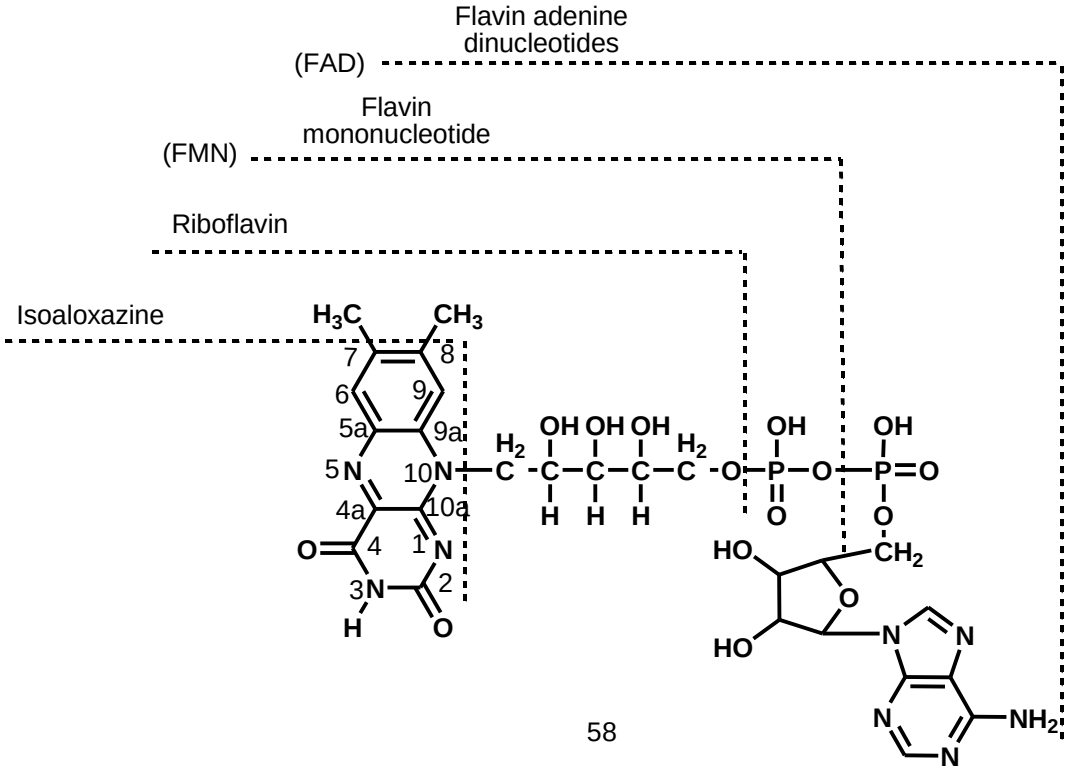

Figure 26. The structure of flavin species and the numbering system for isoalloxazine[91]

The isoalloxazine moiety of the flavocoenzyme is responsible of the various biological activities of flavoproteins. The isoalloxazine exists in three redox states: the oxidized or quinone state, the one-electron reduced or semiquinone (radical) state and the two-electron or hydroquinone state. Since flavin is an amphoteric molecule it presents as neutral, anionic and cationic species in all three redox states.

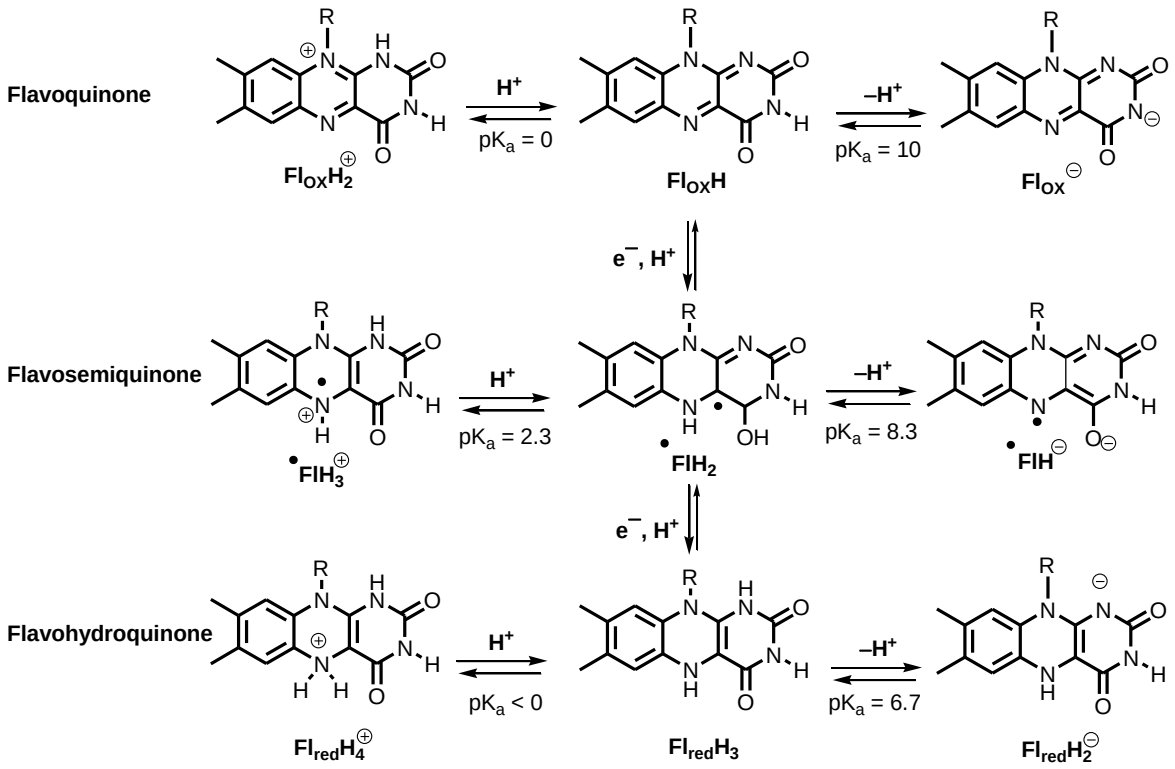

Scheme 6. The structures of the neutral, anionic and cationic flavin species in the three redox states[92].

1.5 Contemporary applications of flavins in materials chemistry.

Due to the fascinating optical and redox properties that flavins possess, they have found numerous applications. For example an optical transistor device based on photo-induced proton transfer reaction has been fabricated from thin-films of the 7,8-dimethylalloxazine on conductive SnO_2 glass. It has been found that when the electrode is illuminated, the cathodic current is improved. During the phototautomerization, the excited tautomer creates two emission bands which are dependent on the pH, as they shift to a shorter wavelength at a high pH[93].

Flavin **59** with the desired excited electronic state properties has proven to be a promising candidate for applications as nonlinear optical devices, molecular electronics applications, or for DSSCs (Figure 27)[94]. In addition, a study on donor–acceptor dyad **60** using a flavin moiety as a photo-active acceptor has exposed a multi-path energy and electron transfer process with a very high transfer efficiency and suggested the flavin is a promising photo-active acceptor candidate for solar energy conversion and storage (Figure 28)[95]

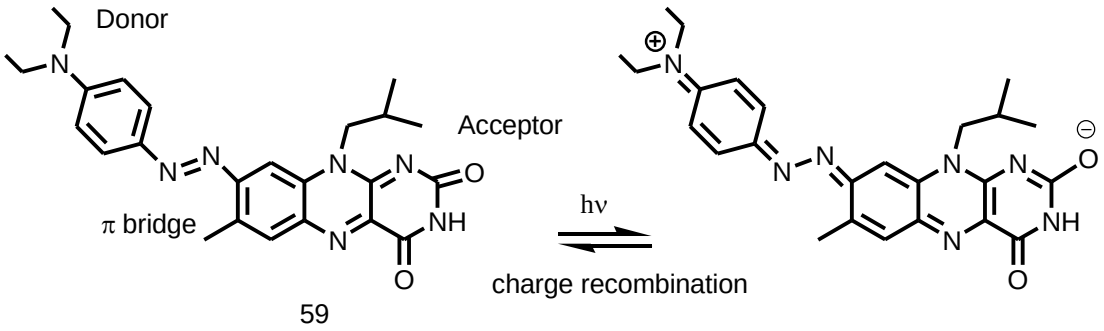

Figure 27. Neutral (left) and charge separated (right) forms of azobenzylflavin[94]

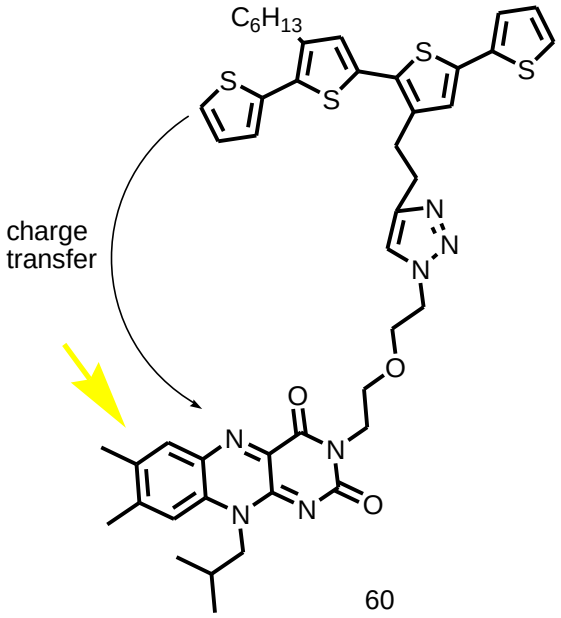

Figure 28. The charge transfer processes when flavin is excited[95]

Porphyrin which is considered as a highly efficient sensitizer for DSSCs[96] has been linked to the flavin via either the N(3) or N(10) positions in two model systems compound **61** and **62.** The flavin reduction potentials were positively shifted by the proximity of the linked porphyrin moiety (Figure 29-a)[97]. Moreover, naphthalenediimide (NDI) unit has also been linked to the flavin through a short spacer group by either the N(3) or N(10) positions and compounds **63** and **64** have been shown to be able to accept multiple electrons. This made them promising acceptor molecules for organic photovoltaic systems (Figure 29-b)[98].

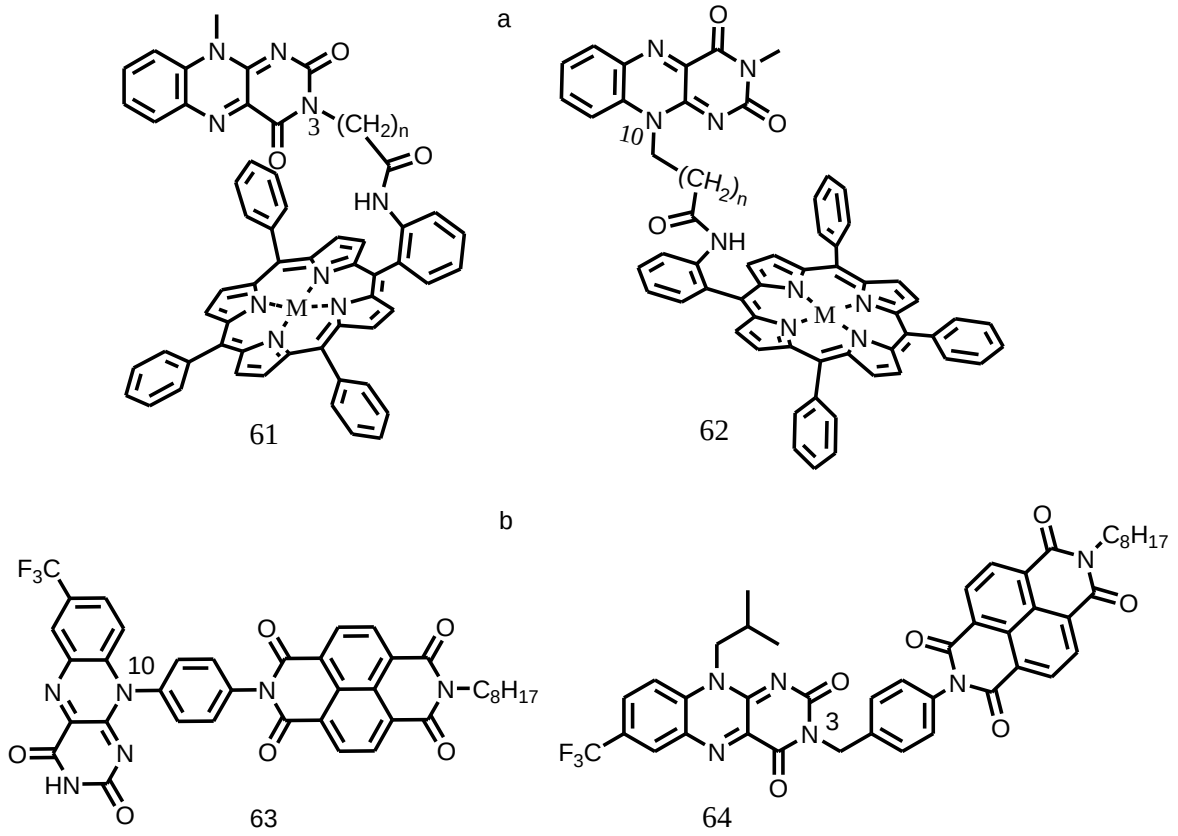

Figure 29. a) Flavin linked Porphyrin model systems[96]. b) Flavin linked naphthalenediimide (NDI) unit[98]

Theoretical calculations of functionalized flavin **65** and its Pt(II) complex **66** (Figure 30-a) suggested that the charge-separated state contributed to the faster quenching from the $^1\pi$-π^* emission state[99]. The photo-dynamics in the pyrene-flavin (isoalloxazine) dyad **67 (**Figure 30-b**)**, is speeded up for both the flavin and the pyrene chromophores because of mutual interaction (energy transfer and charge transfer), opening its application in ultra-fast all-optical logic devices employing high-speed fluorescence dynamics and excited-absorption dynamics. It has been shown that the excitation of the long-wavelength absorbing flavin part led to electron-transfer from the ground-state of the pyrene moiety to the isoalloxazine moiety which causes the fluorescence quenching. Whereas short-wavelength irradiation led to the excitation of both building blocks and caused excited-state electron transfer from pyrene to isoalloxazine, and Forster-type energy transfer from pyrene to flavin followed by ground-state electron transfer from pyrene to flavin[100].

a

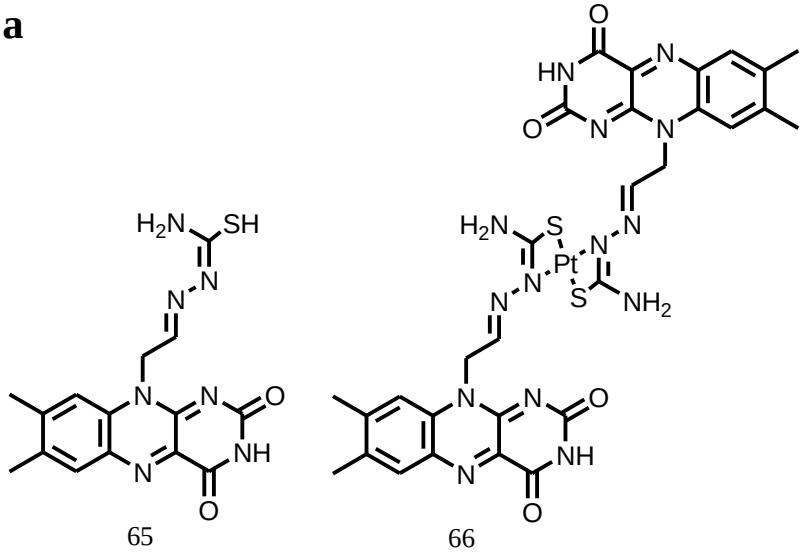

65 66

b

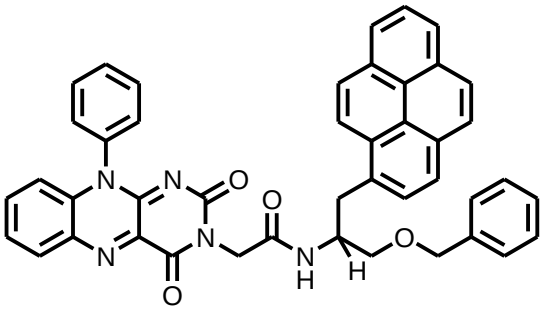

67

Figure 30. a) Functionalized flavin 65 and its Pt(II) complex 66[99]. b) Pyrene-flavin (isoalloxazine) dyad 67[100].

2. Aim of the project

This research programme aims to synthesise new viologen derivatives **70** and **71** (Figure 32). In addition attempts to produce the new ligands **68** and **69** for the formation of ruthenium complexes for DSSC fabrication are also described (Figure 31).

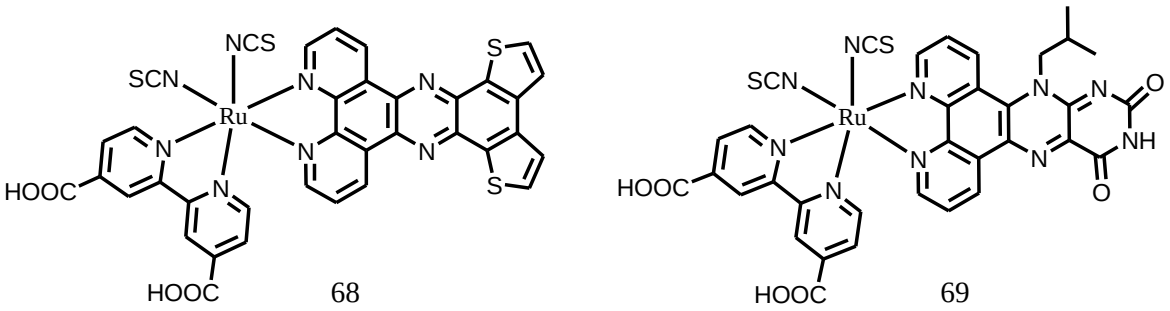

Figure 31. The new Ru(II)-complexes

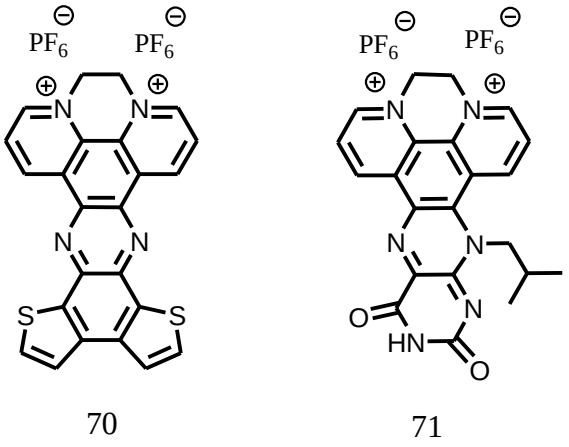

Figure 32. Novel viologen compounds connected to both thiophene 70 and to flavin 71

3. Results and discussion

3.1 Synthesis of materials

Two novel viologen derivatives connected to both thiophene **70** and to flavin **71** were aimed to be synthesised. The molecular structures of these compounds are shown in Figure 32.

3.1.1 Synthesis of compound 70

Initial research focused upon the synthesis of viologen derivatives **70**. The overall synthesis of compound **70** is shown in Scheme 7.

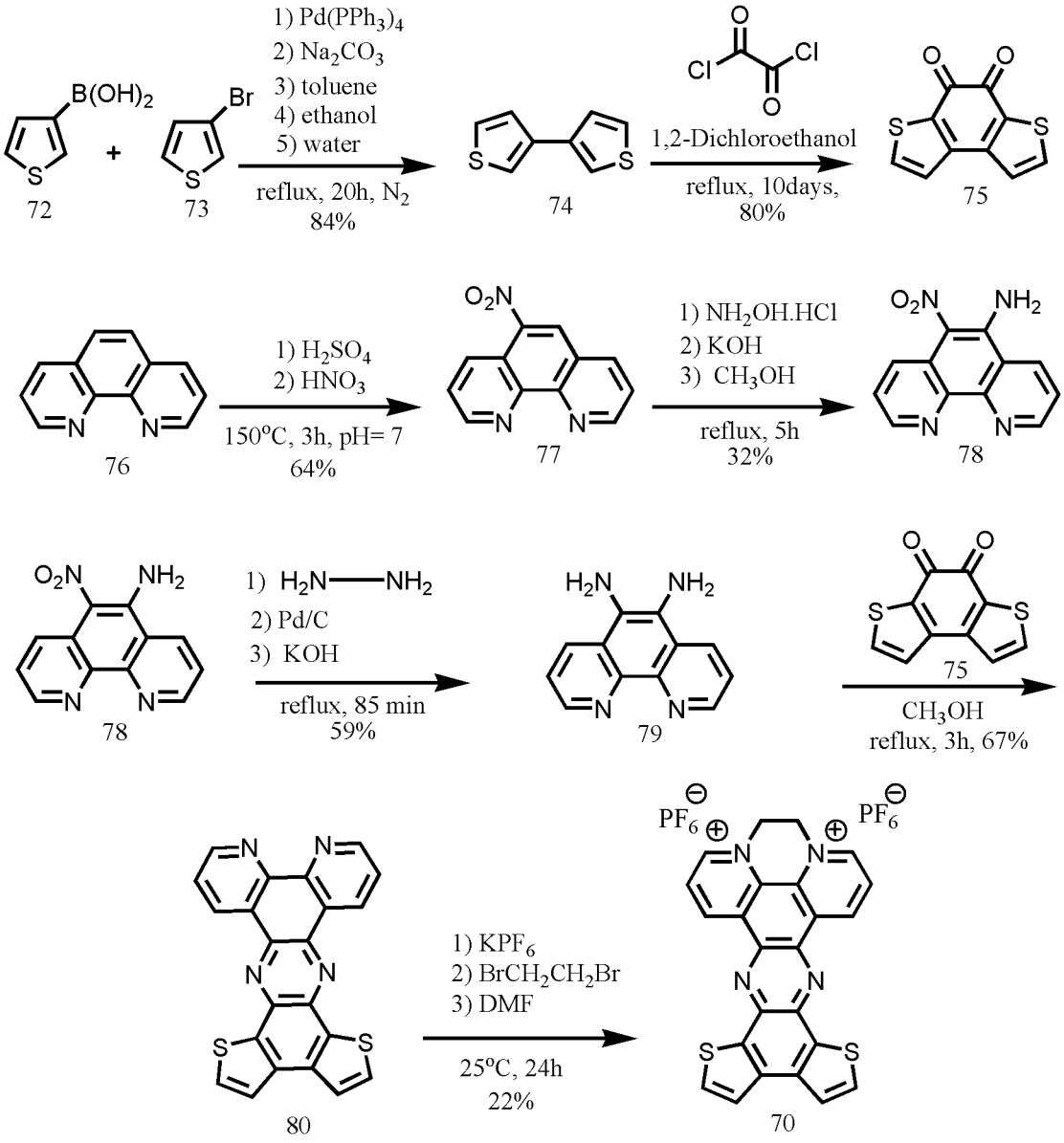

Scheme 7. Methodology for preparing compound 70

The bithiophene **74** was synthesised starting from commercially available 3-bromothiophene **73** and boronic acid **72** by a Suzuki cross coupling reaction[27]**(** Scheme 8**).** 3,3'-Bithiophene **74** was obtained in a good yield.

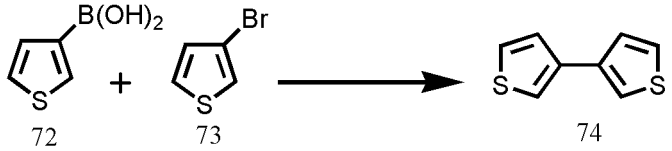

Scheme 8. Synthesis of 3,3'-bithiophene 74

The reaction mixture was deoxygenated by nitrogen bubbling and the reaction was carried out in the presence of tetrakistriphenylphosphine palladium and aqueous sodium carbonate. The purification was carried out by passing the crude mixture through silica column to yield 84 % of 3,3'-bithiophene compound **74**. The mechanism for the formation of **74** is illustrated in Scheme 9.

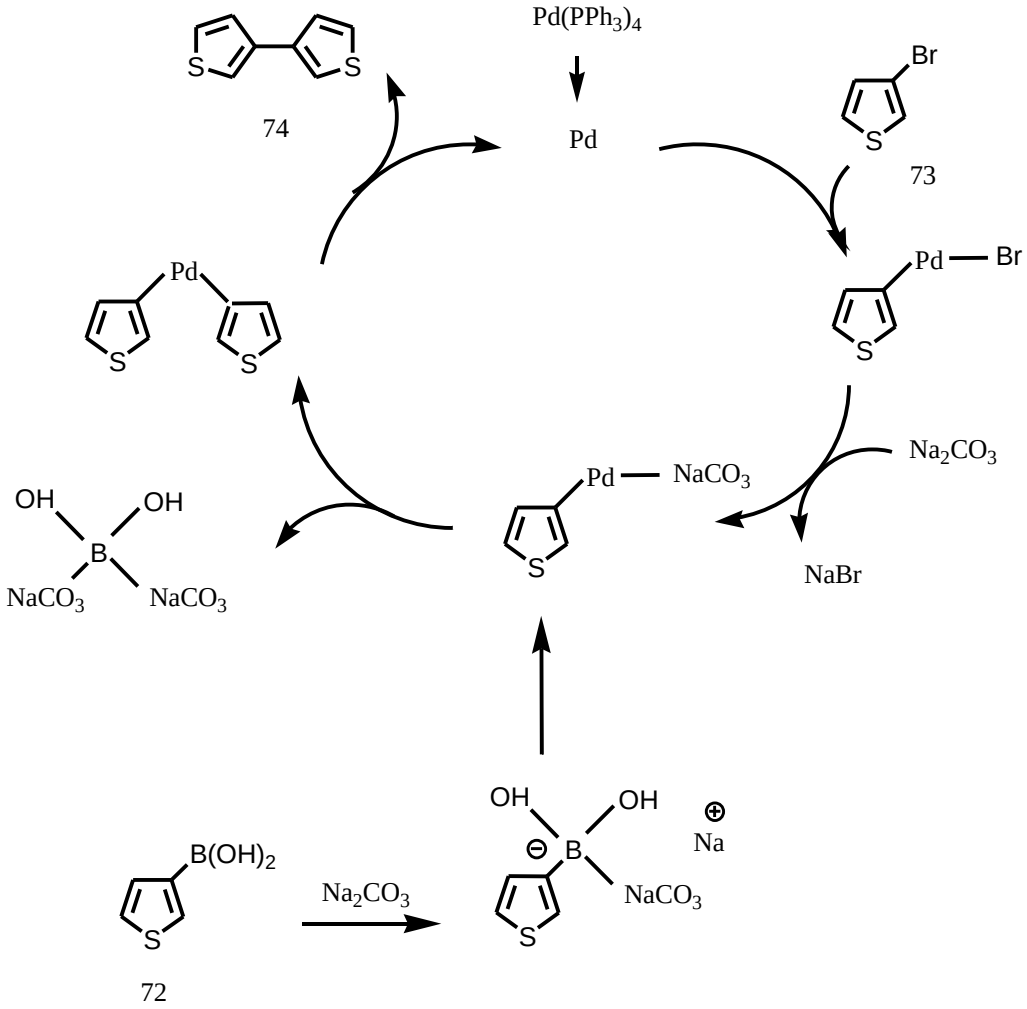

Scheme 9. Mechanisim of synthesising compound 74

The diketone **75** was prepared by two-fold acylation with oxalyl chloride[27]. The reaction took 10 days under reflux and a red powder **75** was collected in 80 % yield (Scheme 10).

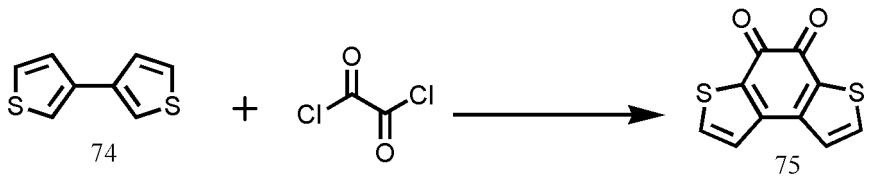

Scheme 10. Synthesis of diketone 75

Nitration of 1,10-phenanthroline **76** to yield compound **77** (Scheme 11) occurred by treating compound **76** (1,10-phenanthroline) with concentrated nitric acid and concentrated sulphuric acid under reflux to yield nitrophenanthroline **77** in 64 % yield.

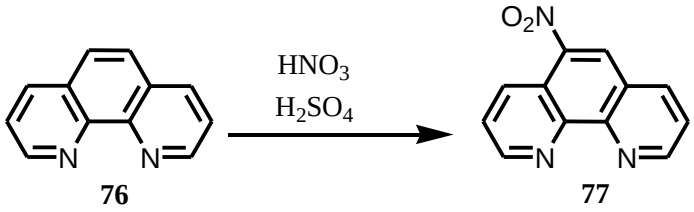

Scheme 11. Synthesis of nitrophenanthroline 77

5-Amino-6-nitro-1 ,l0 -phenanthroline **78** was prepared by direct nucleophilic amination of nitrophenanthroline **77** with hydroxylamine in the presence of KOH (Scheme 12). The lack of solubility of compound **77** in water allows it to be precipitated to yield a brown powder of compound **78** which was used without further purification. The mechanism of the nucleophilic addition is illustrated in Scheme 13.

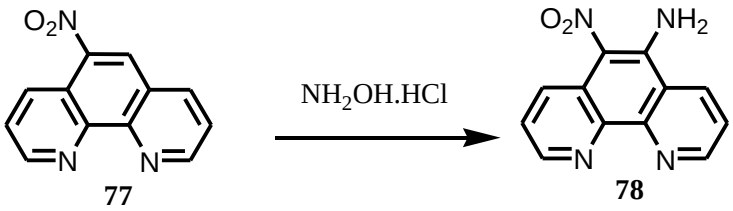

Scheme 12. Synthesis of compound 78

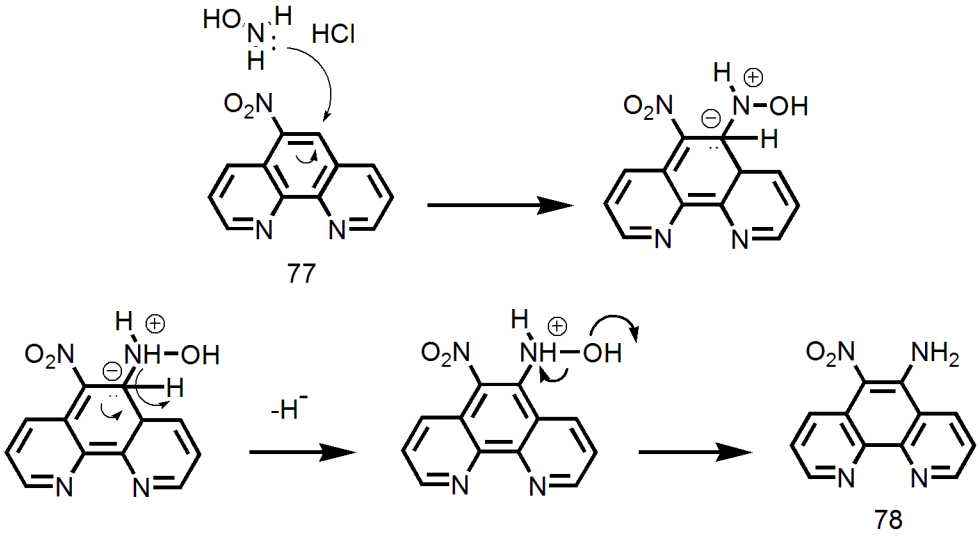

Scheme 13. Nucleophilic aromatic substitution

Reduction of compound **78** by hydrazine/palladium on carbon gave 5,6-diamino- 1,10-phenanthroline **79** in 59 % yield (Scheme 14). No further purification was undertaken due to instability of compound **79**.

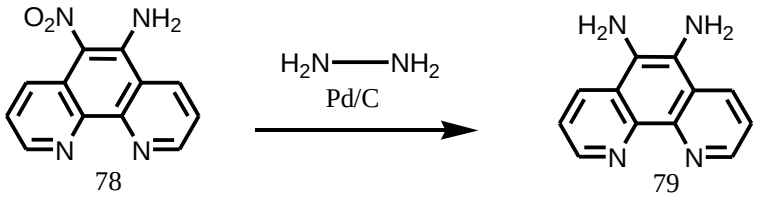

Scheme 14. Synthesis of compound 79

A condensation reaction between the diketone **75** and the diamine **79** in methanol at 67^{o}C gave compound **80** as pale yellow powder in 67 % yield (Scheme 15). Compound **80** was purified by recrystallisation from ether.

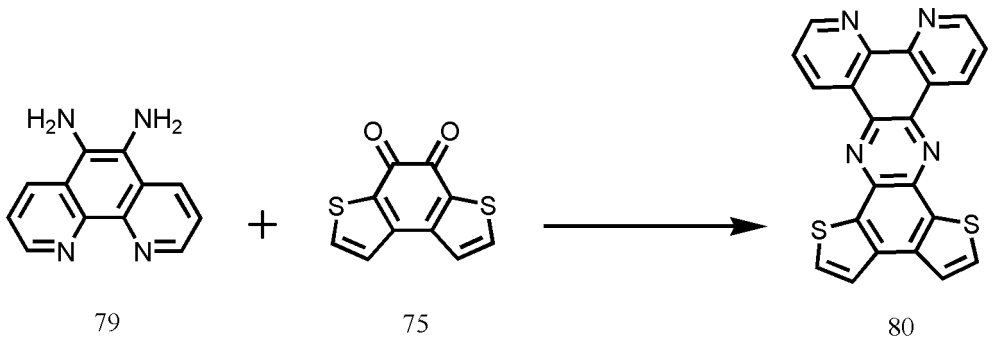

Scheme 15. Synthesis of compound 80

The viologen **70** was prepared from the bipyridine compound **80** using 1,2-dibromoethane. The dibromide salt of **70** was converted to the PF_6^- to improve solubility in organic solvents by reacting with KPF_6 (Scheme 16).

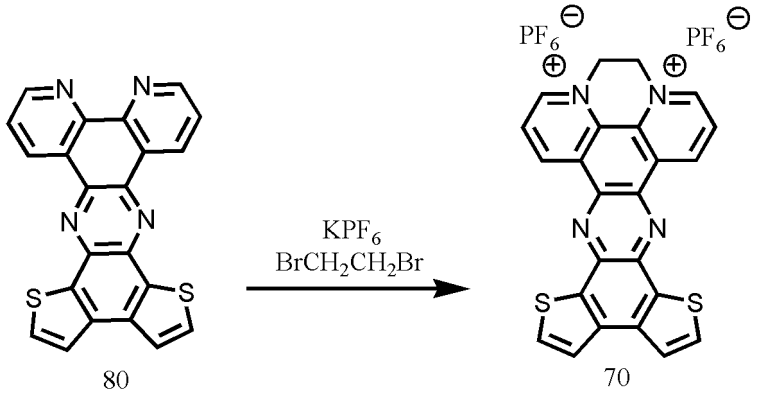

Scheme 16. Synthesis of compound 70

3.1.2 Attempted Synthesis of compound 71

The attempted synthetic protocol to afford compound **83** and **71** is shown in Scheme 17.

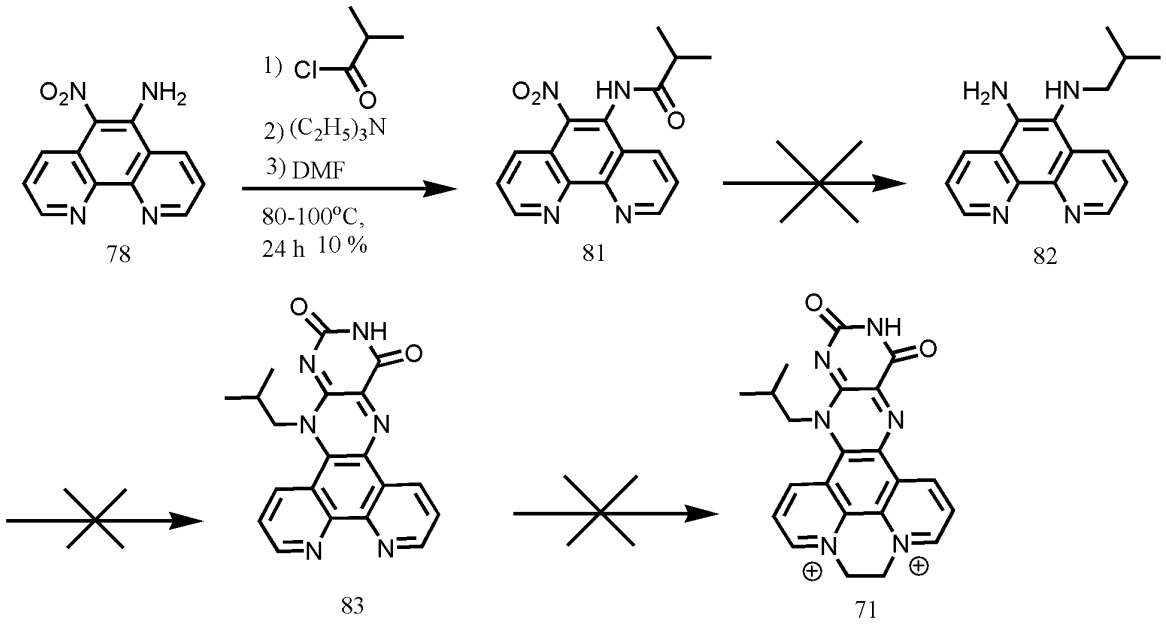

Scheme 17. Attempted methodology of preparing compound 71

Compound **81** was synthesised in 10 % yield by the reaction between compound **78** and isobutyryl chloride in the presence of triethylamine. The addition-elimination mechanism involves the reaction of nitrogen's lone pair on the amine and followed by chloride ion elimination. The presence of triethylamine is to neutralize the hydrochloric acid that was formed during the reaction (Scheme 18).

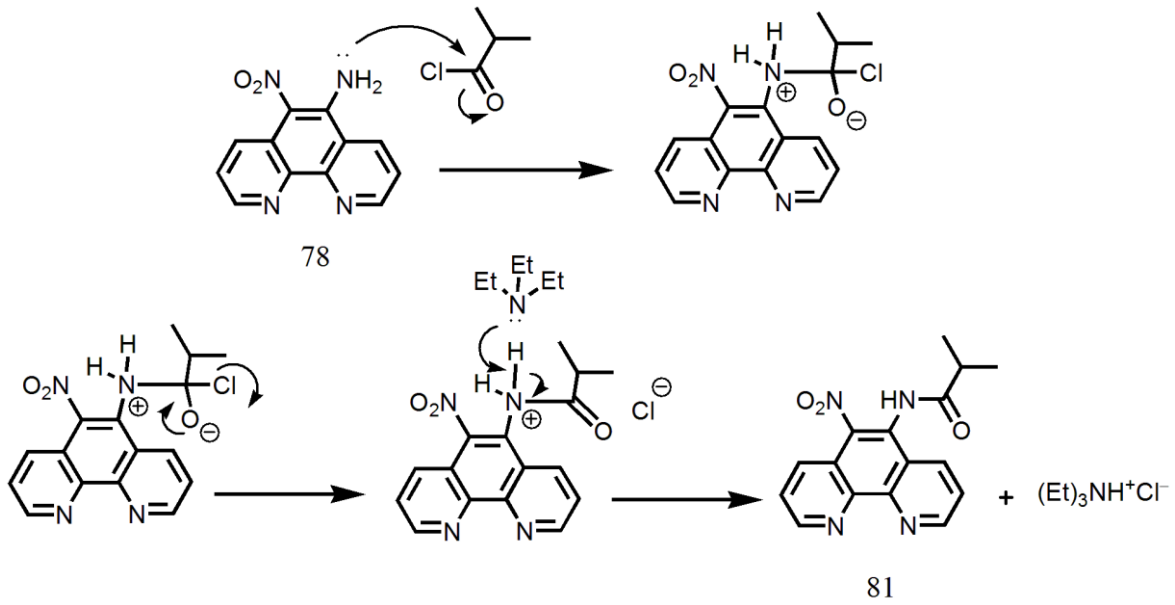

Scheme 18. Mechanism of the acylation process of compound 81

Unfortunately, the acylation of the amine group of **78** proved very difficult and was only successful on one occasion. A range of conditions were tried as shown in Table 1. The lack of reactivity is presumably due to the adjacent electron withdrawing nitro group preventing the electron pair of the amine to undergo nucleophilic attack on the carbonyl group. The synthesis of compound **82** was therefore abandoned.

Table 1. The number of the attempts and multiple conditions that have been changed in the acylation reaction.

No	Solvent	Temp.	Time	atm.	Results
1	DCM	r.t	24 h	O_2	S.M.*
2	DCM	r.t	24 h	N_2	S.M.*
3	Toluene	70-80	24 h	O_2	S.M.*
4	DMF	120-130	24 h	O_2	S.M.*
5	DMF	120-130	24 h	N_2	S.M.*
6	dry DMF	120-130	24 h	N_2	10%
7	dry DMF	120-130	72 h	N_2	S.M.*

*S.M. = Starting materials.

3.2 Characterization of compounds

3.2.1 NMR Spectroscopic studies.

The spectroscopic data of all synthesized compounds are in agreement with the proposed structures. The ^{1}H NMR spectra confirmed the expected signals of the compound **80** and viologen **70.** Due to differences in the solubility, the ^{1}H NMR spectra for the compound **80** was recorded in $CDCl_3$ while the ^{1}H NMR spectra of compound **70** was recorded in DMSO. The positions of the key protons are shown in the Figure 33. Converting of the phenanthroline to the corresponding viologen resulted in shifting of protons to higher chemical shifts due to quaternisation of the phenanthroline nitrogen. For compound **70** the methylene protons adjacent to the positively charged nitrogen at 5.76 ppm (f) are diagnostic.

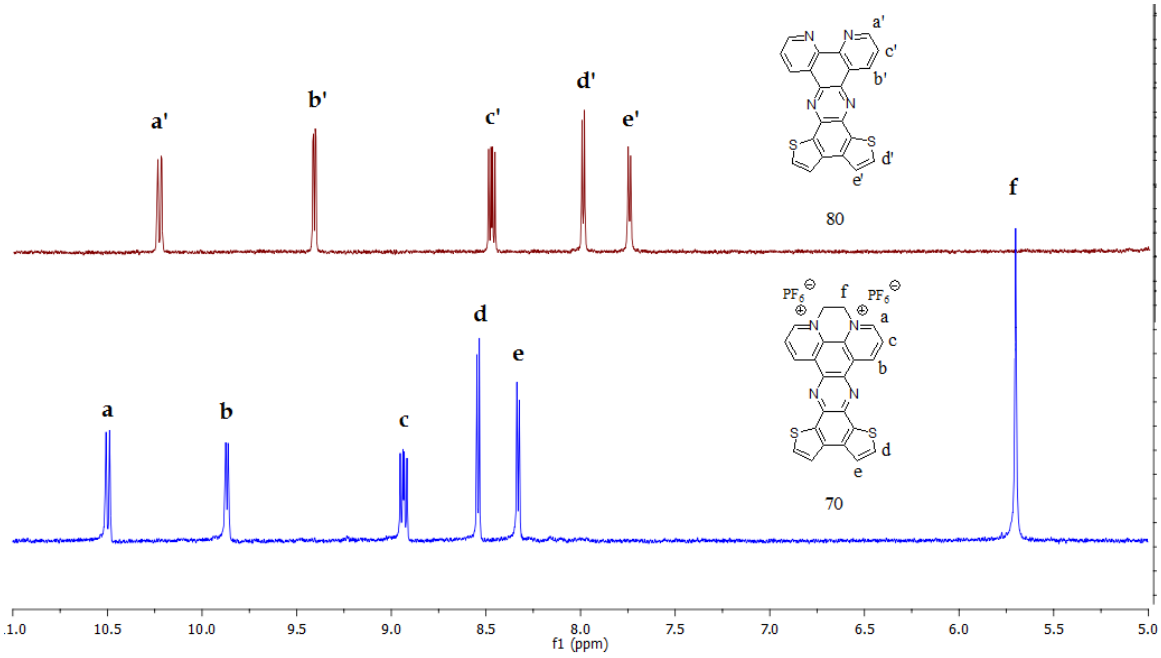

Figure 33. Partial ^{1}H NMR spectra for compounds 70 (blue spectra) and 80 (red spectra)

3.2.2 UV-Visible Studies.

UV-Vis spectra for compound **80** and **70** were recorded in (1 x 10^{-5} M) DMSO. The spectra are shown in Figure 34. The associated data is summarised in Table 2. Despite compounds **70** and **80** displaying similar peaks at 320 nm, 420 nm and 440 nm, new shoulder at 660 nm was observed for compound **70**. This illustrates the influence of the viologen unit on lowering the band gap from 2.07 eV to 1.52 eV on going from **80** to the viologen **70** respectively.

Table 2. UV-Vis spectroscopy data of compounds 80 and 70 (1x10^{-5} M) DMSO

Compounds	λ^1	λ^2	λ^3	λ_{max}	E_{gap} **ev**
80	318	420	440		2.07
70	320	416	440	660	1.52

λ – Maximum absorption wavelength of each peak (nm)

E_{gap} – Gap energy (ev) = h C / λ

Where: h = Planck's constant = 6.626 x 10^{-34} Joule sec

C = Speed of light = 3.0 x 10^{8} metre / sec

λ = Cut off wavelength = (nm x 10^{-9}) metres

Conversion factor 1eV = 1.6 x 10^{-19} Joules

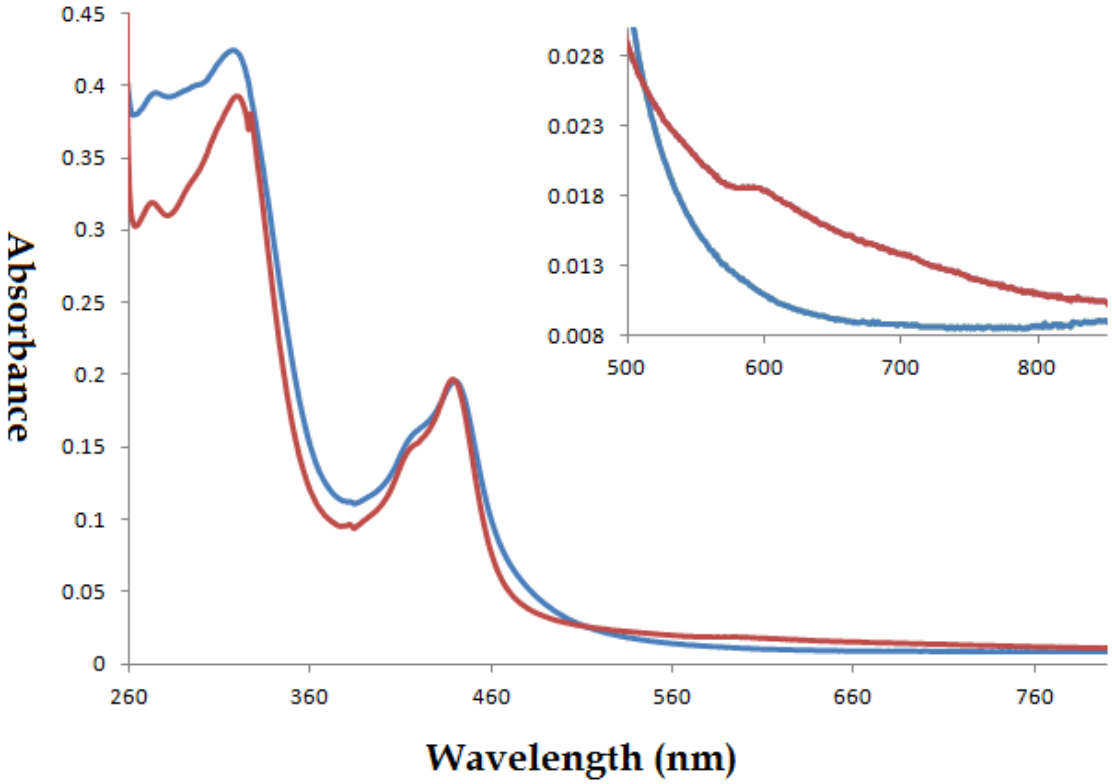

Figure 34. UV-Vis spectroscopy of compound 80 (blue line) and compound 70 (red line) in DMSO ($1x10^{-5}$ M).

3.2.3 Density functional theory (DFT) Calculations

DFT calculations predicted a planar structure for the heterocyclic component of compound **70**. The predicted HOMO and LUMO maps are presented in Figure 35. The HOMO is largely located over the electron rich thiophene units, whereas the LUMO is located over the viologen units as anticipated. The electrostatic potential map (Figure 36) clearly shows that the viologen moiety is more electropositive than the thiophene-based moiety, as expected for a structure of this type.

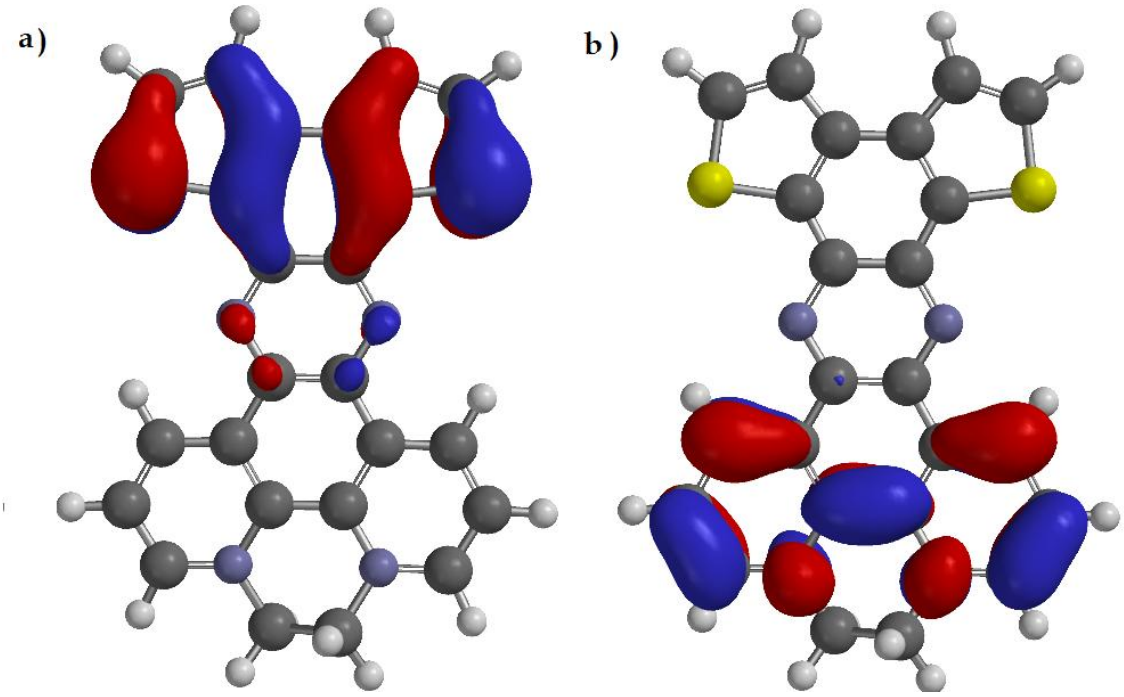

Figure 35. Predicted DFT map for compound 70 a) HOMO b) LUMO

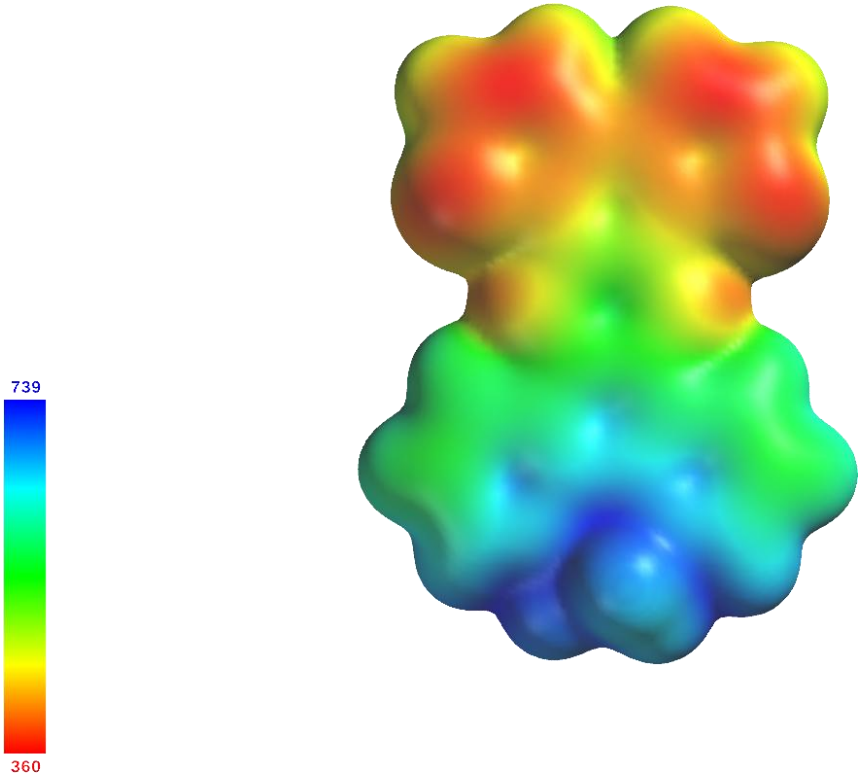

Figure 36. The predicted electrostatic potential map for compound 70

3.2.4 Electrochemical studies

3.2.4.1 Electrochemical studies of monomer 80

Electrochemical properties of compound **80** were examined using cyclic voltammetry. The redox properties of the monomer of compound **80** were performed at room temperature and were carried out in a conventional three electrode cell containing a platinum button as a working electrode, silver wire as a reference electrode and platinum counter electrode. The sample was prepared in (1×10^{-4} M) concentration in DMSO solvent with 0.1 M of tetra-n-butyl ammonium hexafluorophosphate ($TBAPF_6$) as supporting electrolyte and the collected data is referenced to the Fc/Fc^{+} redox couple.

Table 3. Electrochemical data of monomers and oligomers of compound 80.

Compounds	E_{red} (V)	E_{LUMO} (V)	E_{oxi} (V)	E_{HOMO} (V)	E_{gap} (V)
80	-1.06	-3.74	+0.48	-5.28	1.54
Polymer 80	-1.05	-3.75	+0.46	-5.26	1.51

Table 4. Electrochemical data of monomers and oligomers of compound 70.

Compounds	E_{red} (V)	E_{LUMO} (V)	E_{oxi} (V)	E_{HOMO} (V)	E_{gap} (V)
70	-0.94	-3.86	+0.40	-5.20	1.34
Polymer 70	-0.82	-3.98	+0.17	-4.97	0.99

E_{red} - First reduction potential (V)

E_{rev} - First reversible potential (V)

$E_{LUMO} = - 4.8 - E_{red}$ (V)

$E_{HOMO} = - 4.8 - E_{(oxi)}$ (V)

$E_{gap} = E_{oxi} - E_{red}$

Cyclic voltammetry data for compound **80** are fairly complicated (Table 3) and revealed that one reversible reduction wave was observed at $E_{1/2 =}$ - 1.06 V and one quasi-reversible reduction wave at $E_{max =}$ - 1.39 V (Figure 37). The estimated LUMO energy for this compound is – 3.74 V. This compound also showed a weak irreversible oxidation peak within the anodic scan at E_{oxi} = + 0.48 V. This can be attributed to the formation of thiophene radical cation unit. The estimated HOMO level is - 5.28 V. The estimated band gap from the onset of the oxidation and reduction waves is 1.54 V.

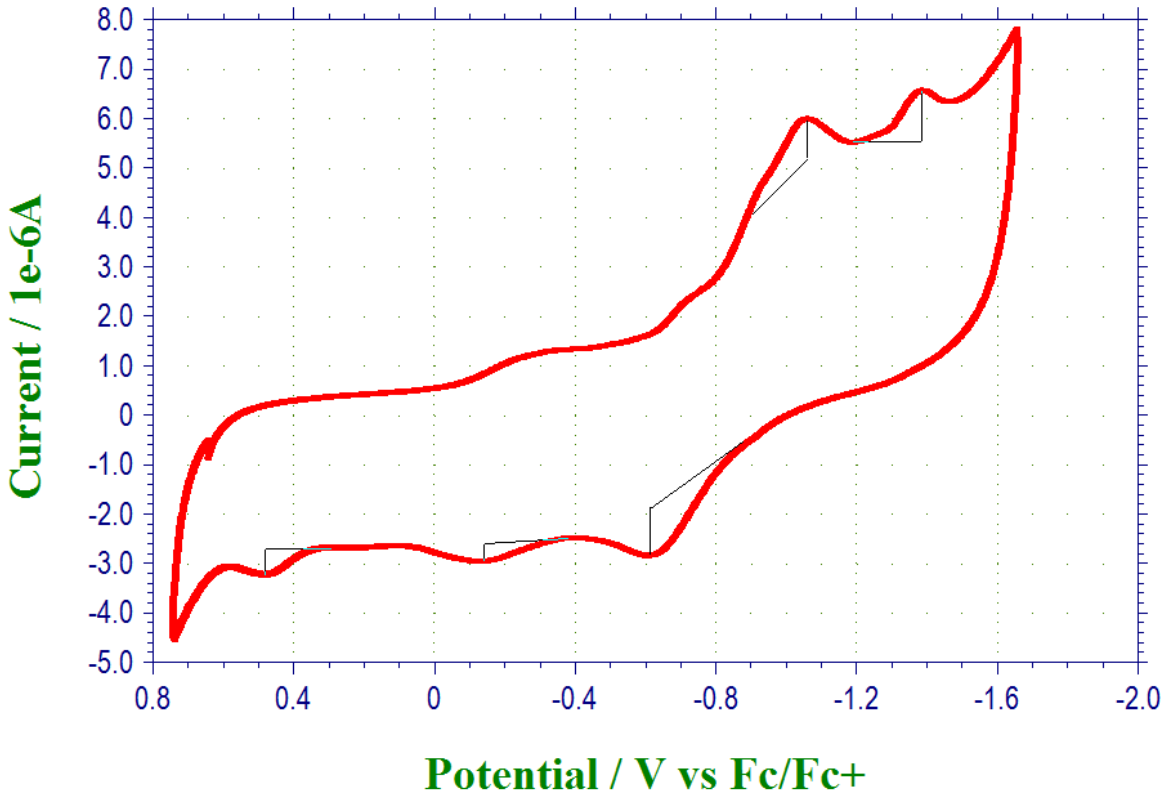

Figure 37. Cyclic voltammetry of compound 80 recorded in DMSO (1x 10^{-4}) solution, with $TBAPF_6$ 0.1 M as supporting electrolyte and at scan rate of 100 mVs^{-1}

3.2.4.2 Electrochemical polymerization of 80

Compound **80** was electropolymerized from solution. The polymerization was carried out using a platinum carbon working electrode, a silver wire reference electrode and a platinum counter electrode using potential dynamic mode. The potential values for the compound are referenced to the potential of the Fc^{+}/ Fc redox couple which was utilized as an internal standard. The growth of the oligomer was accomplished through repetitive redox cycles monitored by cyclic voltammetry. The growth of the oligomers **80** over 600 segments is illustrated in Figure 38**,** which shows an increase in the current with each cycle and a shift of the peaks to a more negative reduction potential corresponding to the formation of a polymer on the electrode surface.

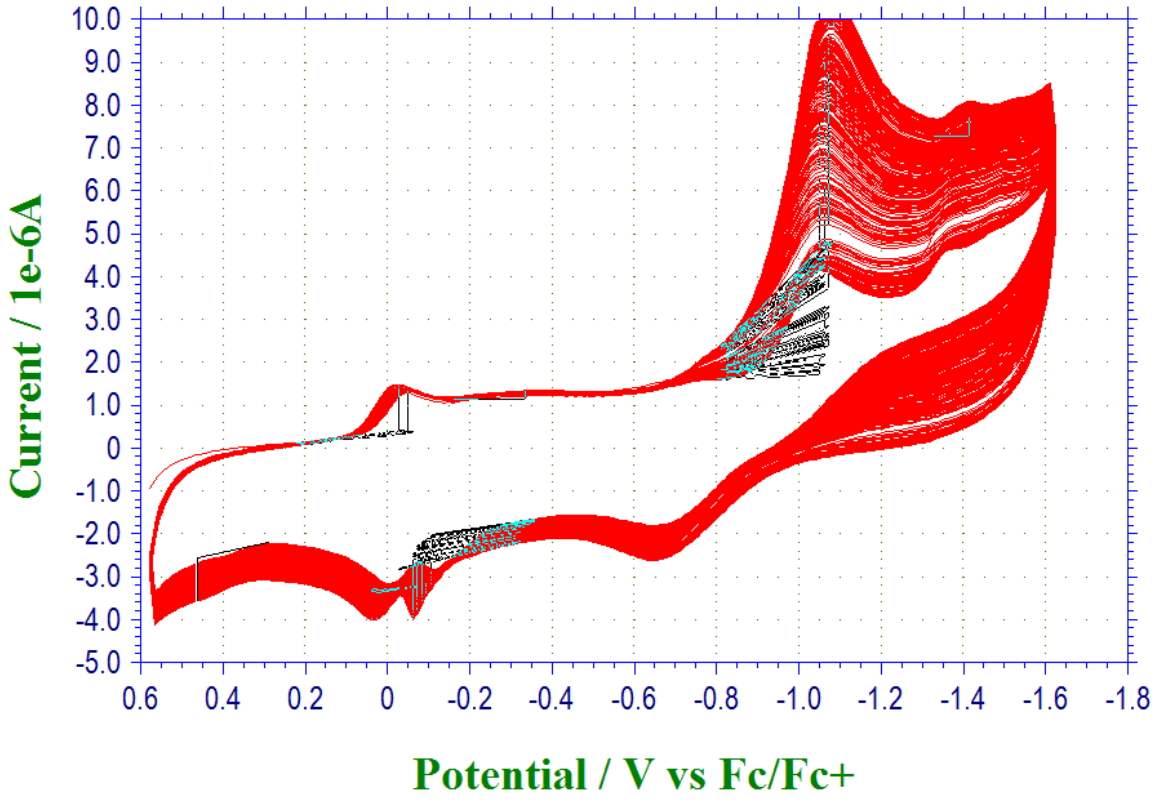

Figure 38. Polymer growth of monomer 80 over 600 segments on platinum working electrode

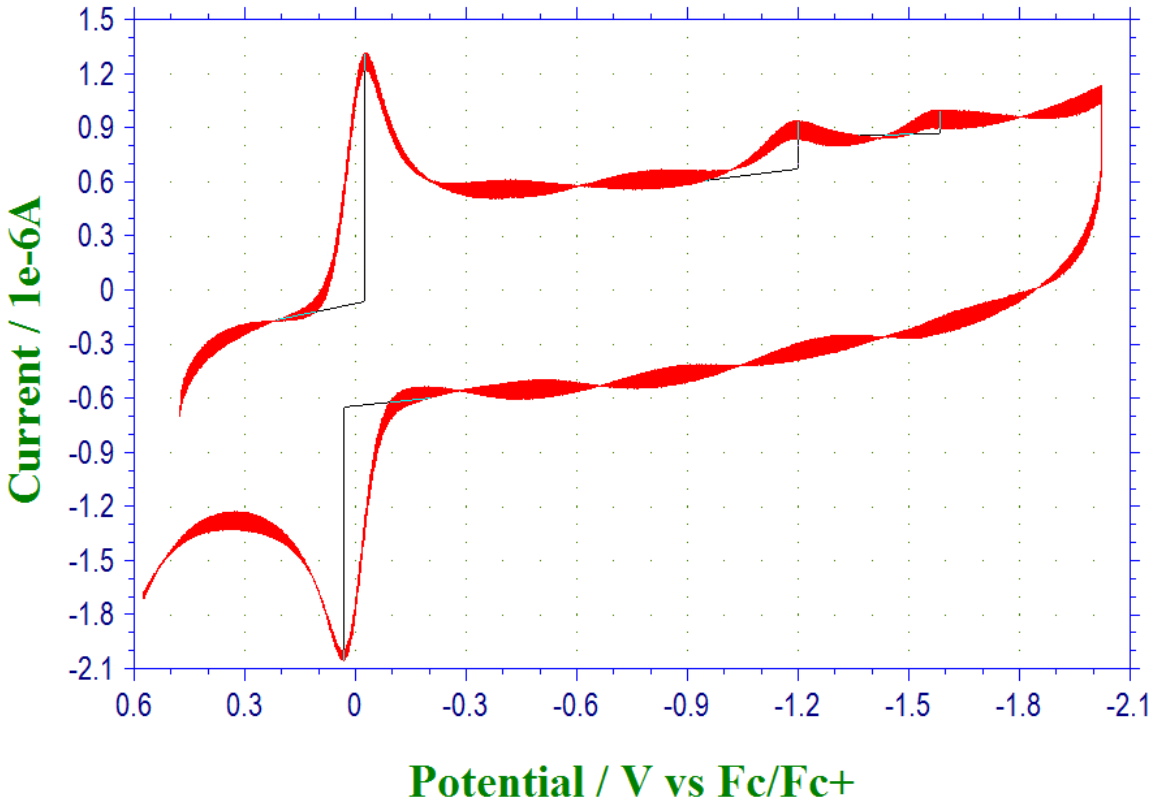

Figure 39. Polymer of monomer 80 scans rate 0.1V/s

The electrochemical properties of the polymer were studied via transferring the coated electrode into a solution of pure electrolyte in DMSO solution (Figure 39). Two quasi-reversible reduction waves at E_{red} = - 1.05 V and at - 1.42 V corresponding to the phenanthrene unit were observed. The E_{LUMO} was calculated to be -3.75 V. The compound showed an oxidation peak within the anodic scan at + 0.46 V. The E_{HOMO} was calculated to be – 5.26 V. The LUMO and HOMO levels provided a lower band gap of 1.51 eV which is slightly lower than monomer **80** further suggesting polymerization occurs.

Repetitive cycling of the deposited film on the working electrode in free of monomer solution has been carried out to explore the stability of the resulting oligomers **80**. The results have indicated that a reasonably stable polymer resulted as the polymer film displayed a linear current relationship upon changing the scan rate. This was determined by plotting the relationship between the scan rates against the maximum current peaks at -1.5 V. The obtained nonlinear relationship is shown in Figure 40.

Table 5. Variable scan rate versus maximum current measurement at -1.5 V for the oligomer formed from monomer 80.

Scan Rate V/s	Current ηA
0.10	0.94
0.15	1.76
0.20	2.20
0.25	2.80
0.35	3.84
0.40	4.34
0.45	4.62
0.50	5.00

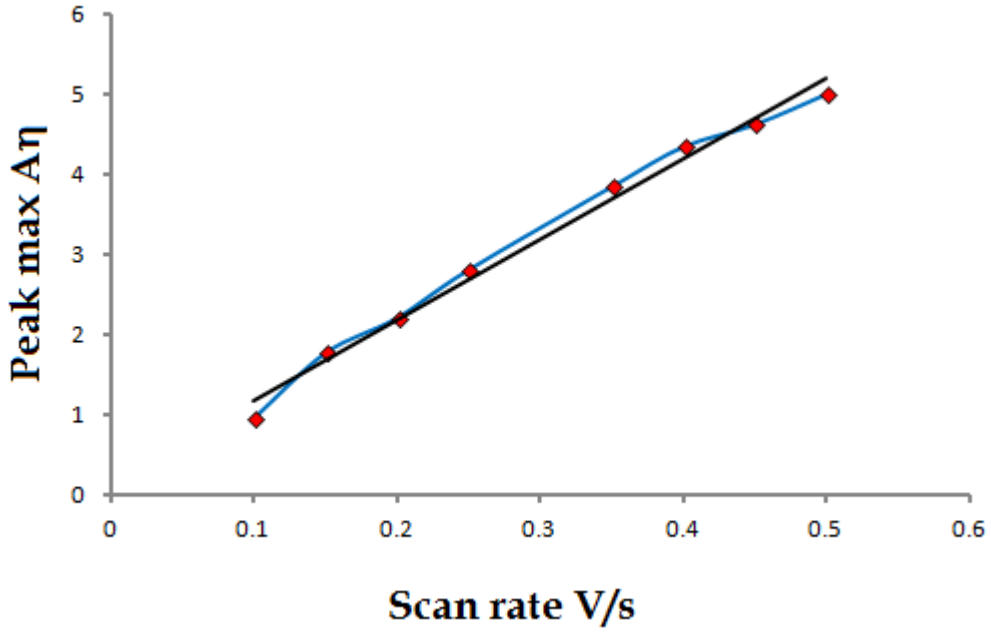

Figure 40. Variable scan rates versus maximum current measurement for the oligomer formed from monomer 80.

3.2.4.3 Electrochemical polymerization of monomer 70

The electrochemical properties of compound **70** were investigated using the cyclic voltammetry. The sample was prepared at room temperature in a solution of (1 x 10^{-4}M) DMSO containing tetra-n-butyl ammonium hexafluorophosphate (Bu_4NPF_6 0.1 M) as supporting electrolyte with a glassy carbon working electrode and a silver wire reference electrode and a platinum counter electrode using potential dynamic mode. The potential was referenced to the Fc/Fc^+ redox couple. The scan rate was 0.1 V/s.

As shown in Figure 41 and Table 3, monomer **70** has one major reversible reduction wave at E_{red} = - 0.94 V presumably corresponding to the two electron reduction of viologen to the neutral species. The anodic scan exhibits one quasi-reversible peak at + 0.40 V (Figure 42). The lower reduction potential of **70** compared to precursor **80** is in line with the predicted better acceptor properties of **70**.

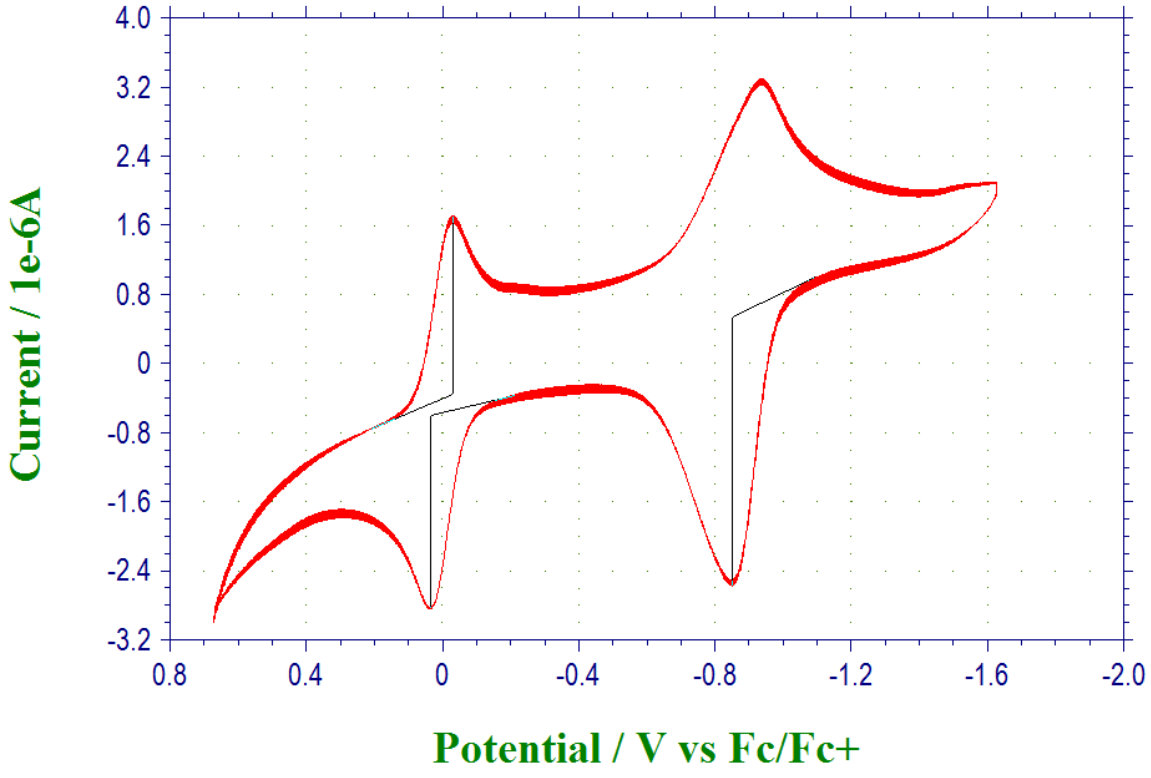

Figure 41. Monomer reduction wave of compound 70 recorded in DMSO (1 x 10^{-4}) solution with $TBAPF_6$ 0.1 M as supporting electrolyte and at a scan rate of 100 mV/s

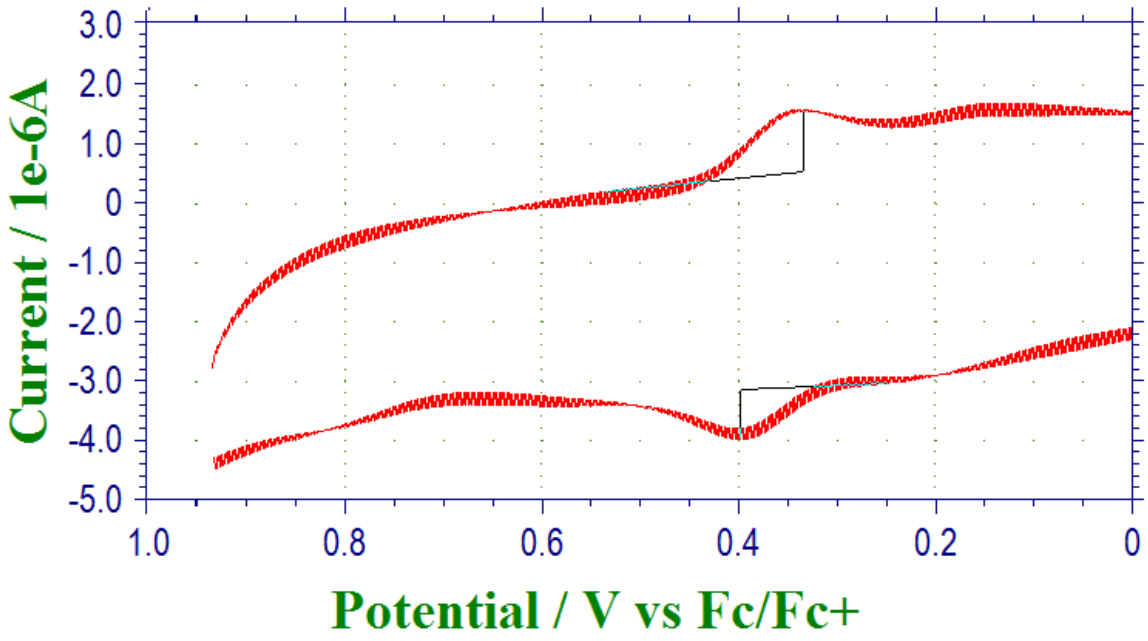

Figure 42. Monomer oxidation wave of compound 70 recorded in DMSO (1 x 10^{-4}M) solution with $TBAPF_6$ 0.1 M as supporting electrolyte and at a scan rat of 100 mV/s

Possible redox states of compound **70** are shown in Scheme 19. The CV studies shown here suggest that in DMSO a single two-electron reduction occurs ($V^{2+} \rightarrow V^{0}$), and the $V^{+\bullet}$ state was not observed.

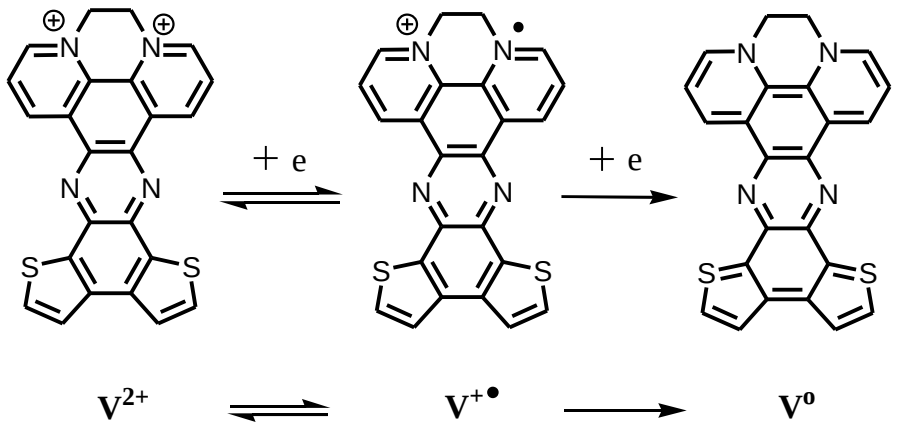

Scheme 19. The possible redox states of viologen 70

3.2.4.4 Electrochemical polymerization of 70

Attempts were made to polymerize monomer **70** from solution. The polymerizations were carried out using glassy carbon working electrode, a silver wire reference electrode and a platinum counter electrode using potential dynamic mode. The Fc^{+}/ Fc redox couple utilized as an internal standard. The growth of the oligomer appeared to be accomplished through repetitive reduction cycles monitored by cyclic voltammetry. The growth of the oligomer **70** over 200 cycles is illustrated in Figure 43 and Figure 44 which shows an increase in the current with each cycle and the development of a new peak at a lower oxidation potential corresponding to the formation of a polymer on the electrode surface. A quasi-reversible oxidation peaks at E= + 0.17 V and a quasi-reversible reduction peaks at E = - 0.82 V were observed for the oligomer of **70**. The approximate electrochemically determined band gap calculated from the oxidation and reduction potentials of the polymer is 0.99 V (Figure 45). Electropolymerization was also carried out by replacing the glassy carbon electrode with ITO slide by transferring the coated electrode into pure DMSO solution using same potential scan (Figure 46).

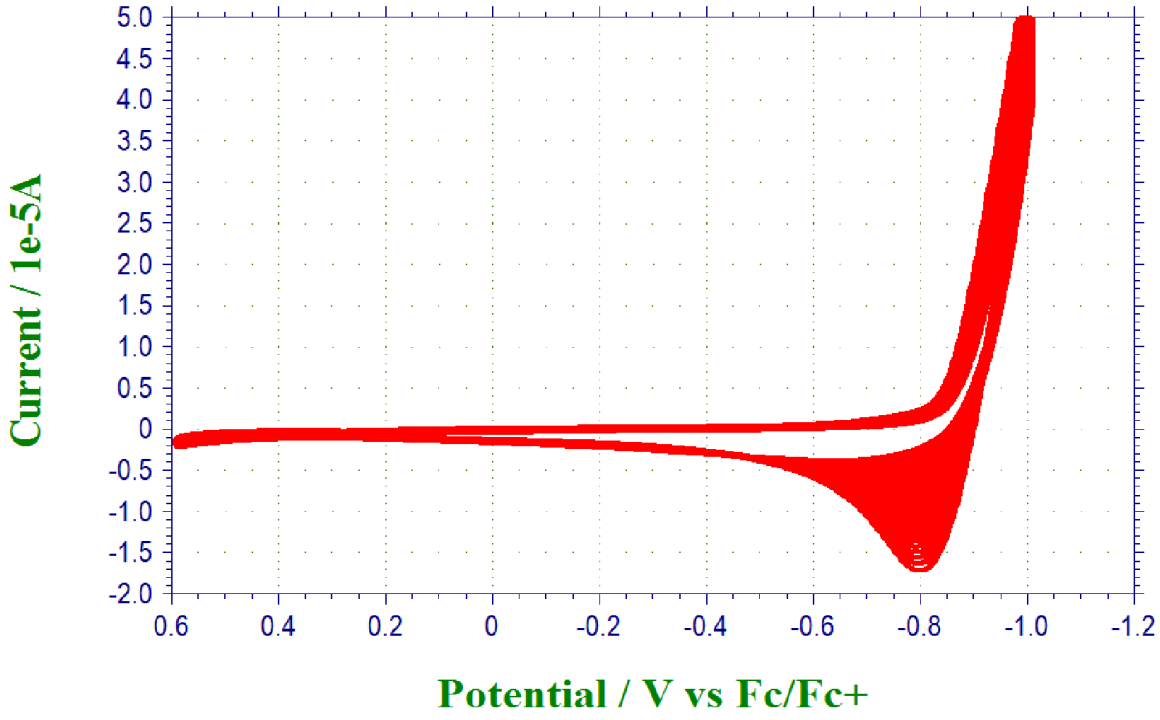

Figure 43. Polymer growth of monomer 70 over 200 segments on glassy carbon as working electrode (cathodic scan)

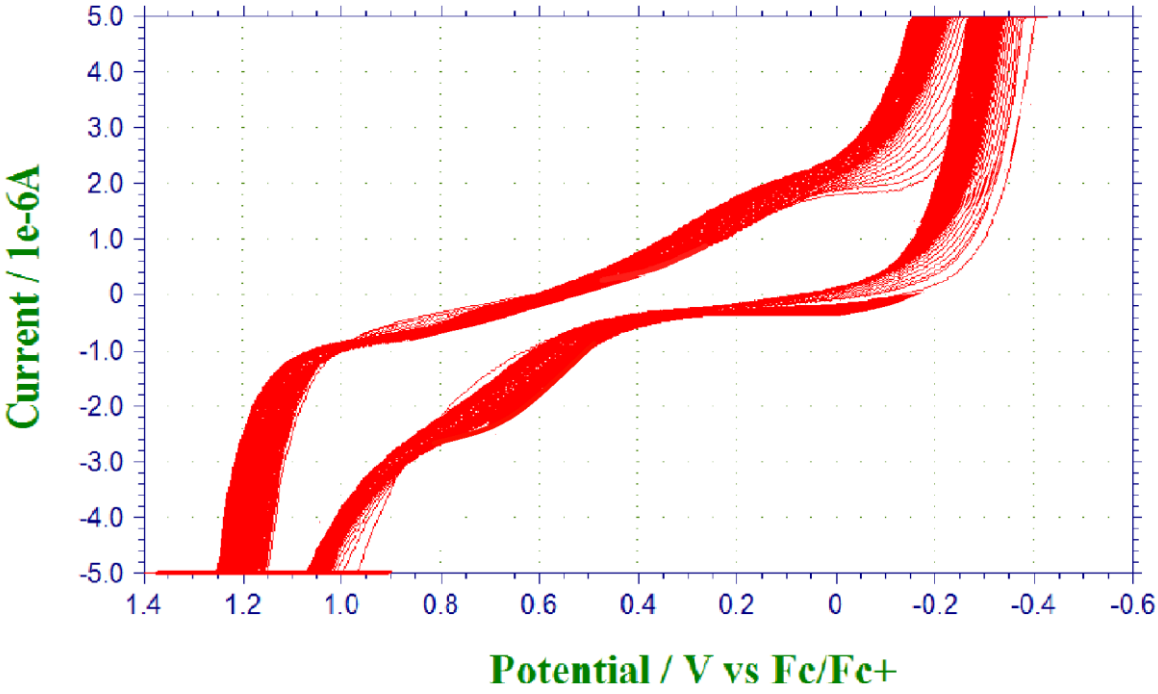

Figure 44. Polymer growth of monomer 70 over 200 segments on glassy carbon as working electrode (anodic scan)

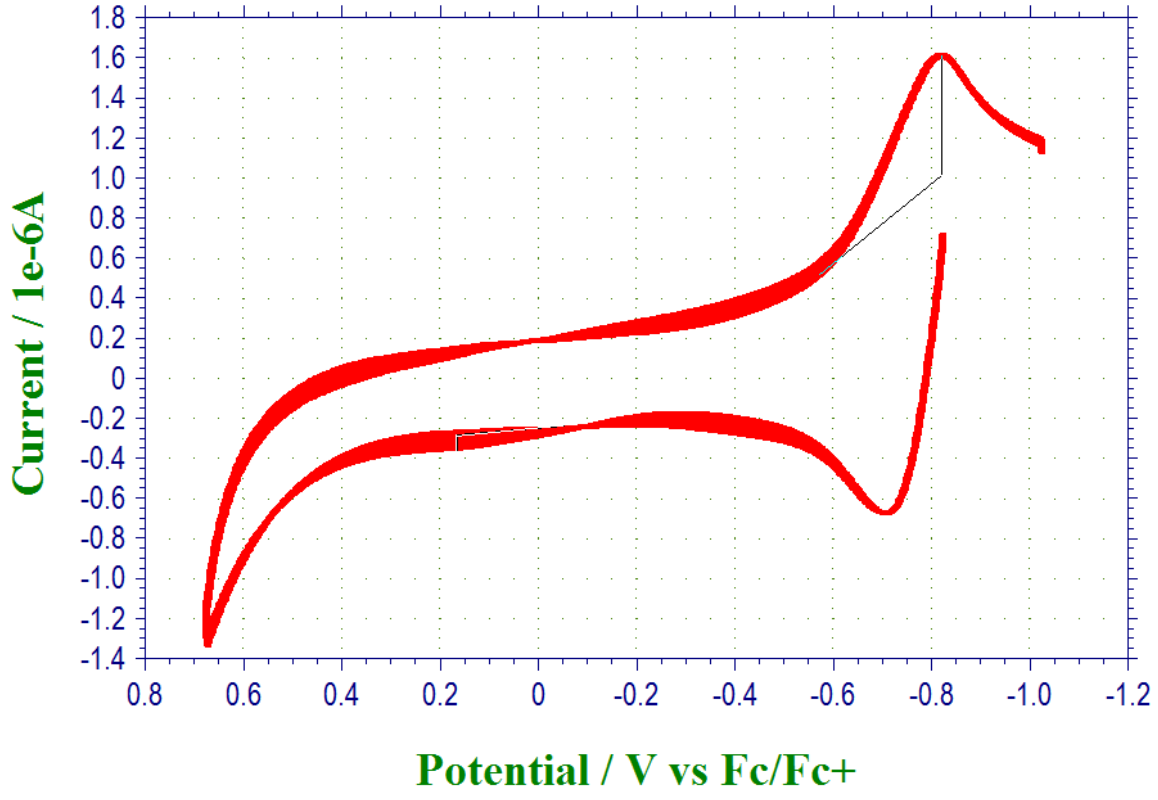

Figure 45. Polymer of compound 70 scans rate 0.1V/s

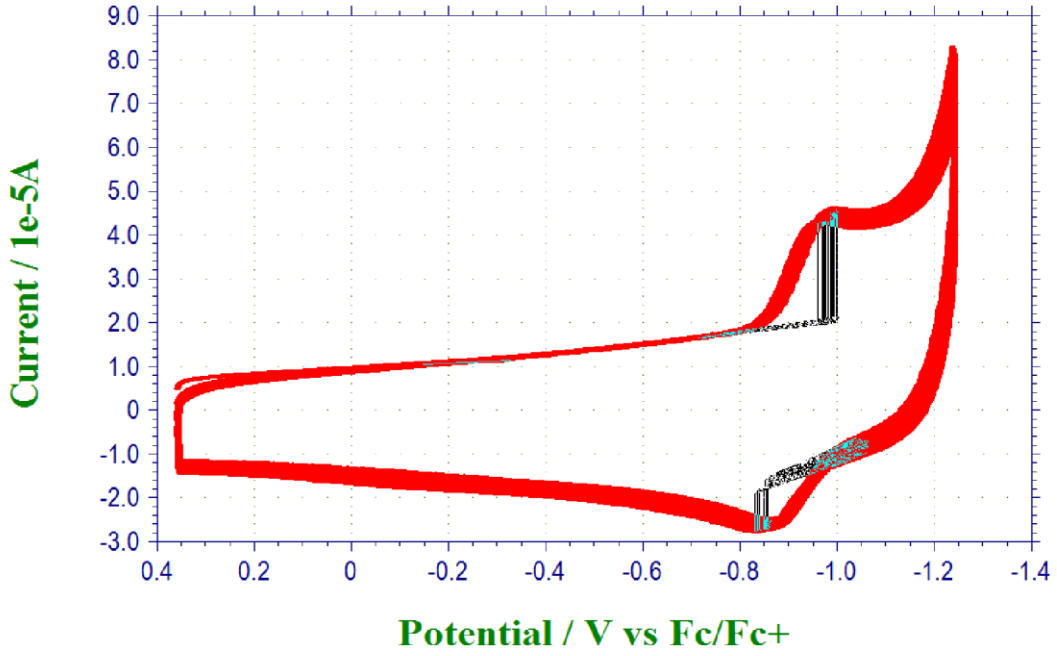

Figure 46. Polymer growth of monomer 70 over 200 segments on ITO as working electrode

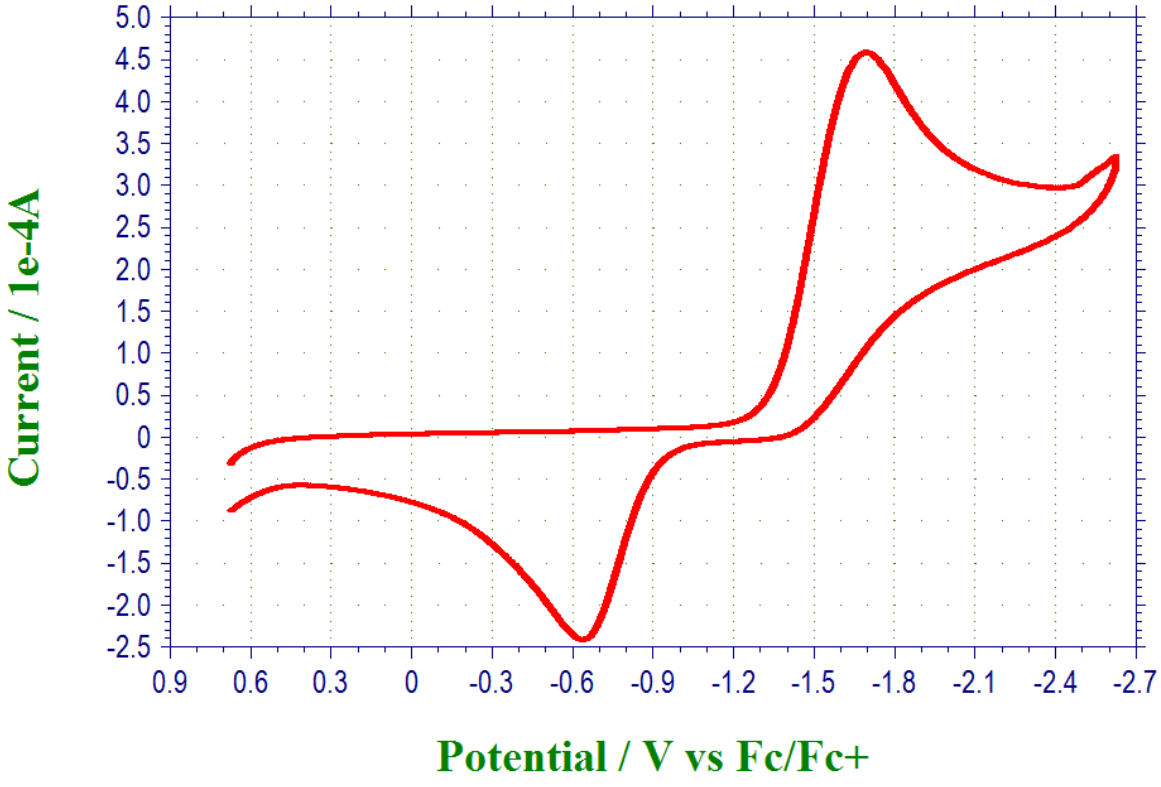

Figure 47. CV reduction scan of oligomer 70 in monomer free DMSO solution

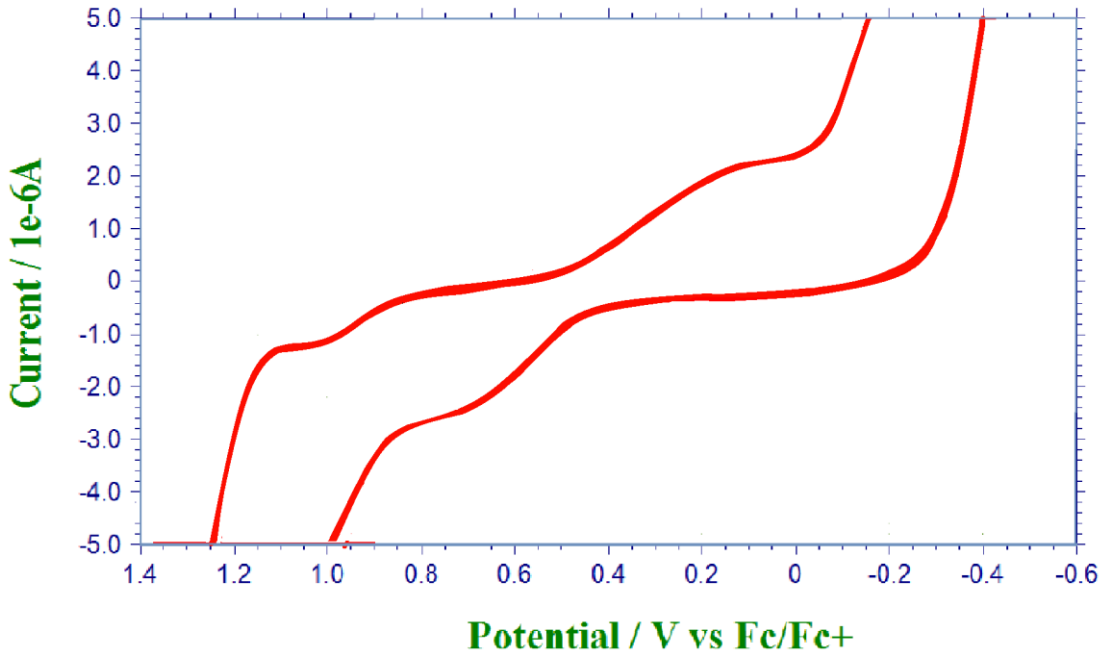

Figure 48. CV oxidation scan of oligomer 70 in monomer free DMSO solution

CV of the polymer films was recorded in monomer- free solution and as shown in Figure 47 and Figure 48.

Thin films of oligomer **70** exhibited reasonably good electrochemical stability upon varying the CV scan rates. This was determined by plotting the relationship between the scan rates against the maximum current peaks at -0.75 V. The obtained linear current vs. scan rate relationship is shown in Figure 49.

Table 6. Variable scan rate versus maximum current measurement at - 0.75 V for the oligomer formed from monomer 70.

Scan Rate V/s	Current ηA
0.10	1.61
0.20	2.65
0.30	3.46
0.40	3.99
0.50	4.64
0.60	5.30
0.70	5.66

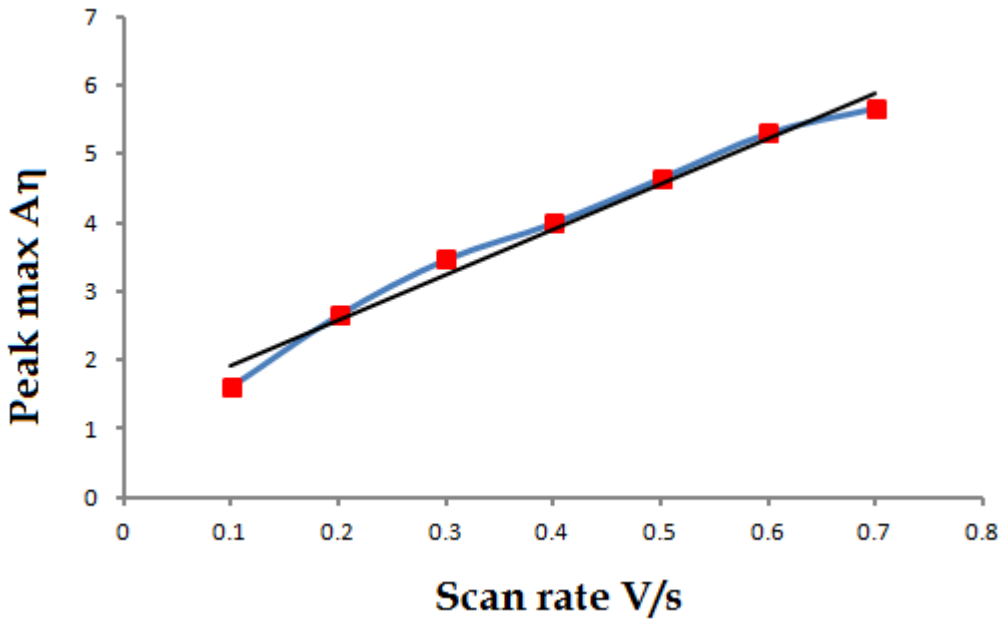

Figure 49. Variable scan rate against current measured for oligomer 70.

4. Conclusion

This thesis describes the successful synthesis of phenanthrene derivative **80** and a viologen analogue **70.** The new compounds have been characterised using UV-vis spectroscopy, cyclic voltammetry, NMR and mass spectrometry. DFT calculations show that the LUMO is located over the phenanthrene moiety, whereas the HOMO is located over the more electron rich thiophene units. Preliminary investigations suggest that both derivatives may be electropolymerised from solution to afford reasonably robust thin films. Future work will involve a more detailed study of the polymerisation process and the properties of the resulting polymers.

Unfortunately the syntheses of compounds **83** and **71** were unsuccessful. Although a range of reduction reactions were attempted to convert **81** to **82**, all were unsuccessful. Therefore a new reaction strategy needs to be developed to avoid the necessity of this reduction step.

5. Experimental

5.1 General

All starting compounds were supplied from commercial sources and were used as received without purification unless stated. Flash column chromatography was carried out using Fisher Matrix silica 60. Macherey-Nagel aluminum backed plates pre-coated with silica gel 60 (UV_{254}) were used for thin layer chromatography and were visualized by ultra violet light.

^{1}H NMR and ^{13}C NMR spectra were recorded on Bruker Avance 400MHz spectrometers with chemical shift values in ppm. Tetramethylsilane (TMS) was used as reference for all NMR spectra ($\delta = 0.0$ ppm)

MS spectra and accurate Masses were obtained from using a JEOL JMS-700 spectrometer. They were measured using FAB conditions by the analytical services in the School of Chemistry, University of Glasgow.

Transmission infrared spectra were recorded on Perkin-Elmer RX FT-IR system.

Electrochemical experiments were carried out using dry DMSO with 0.1 M $TBAPF_6$ as the supporting electrolyte and were recorded using a CH Instruments Inc. (Austin, TX, USA.), 440 a EC Analyser.

UV - Vis absorption spectra were recorded using a Perkin - Elmer Lambda 25 Spectrometer (Cambridge, U.K). All experiments were carried out at ambient temperature using $1cm^3$ quartz cuvettes.

DFT calculations were performed using the Spartan ’14 (64-bit) software suite*. Geometries optimized using DFT (B3LYP/6-31G*), and the resulting structures were shown to be local minima by inspection of their vibrational frequencies.

---

* Wavefunction Inc., 18401 Von Karman Ave., Suite 370, Irvine, CA 92612, USA

5.2 Synthetic experimental

3,3'-Bithiophene (74)[27]

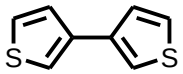

74

Compound **73** (1.64 mL, 17.50 mmol) and 3-thiophene boronic acid **72** (2.5 g, 19.53 mmol) were dissolved in a mixture of toluene (87 mL), ethanol (40 mL) and water (35 mL). Na_2CO_3 (11.17g, 105.4 mmol) was added to the reaction mixture. The solution was heated to reflux (120^oC) under N_2 for 2 h then $Pd(PPh_3)_4$ (0.2 g, 0.175 mmol) was added to the mixture and left under heating overnight. The reaction was cooled to room temperature and extracted with dichloromethane (3 x 100 mL). The organic layer was washed with saturated $NaHCO_3$ and brine. The combined organic extracts were dried over $MgSO_4$, filtered and evaporated. Column chromatography (silica gel/ eluting with DCM / petroleum ether (1:2)) afforded 3,3'-bithiophene **74** (2.2 g, 84%) as colourless crystals. mp. 126-129 ^oC. ^1H NMR (400 MHz, $CDCl_3$) δ = 7.31 (dd, 2H, *J* = 2.8 Hz, 1.5 Hz), 7.27 (dd, 2H, *J* = 8.2 Hz, 5.0 Hz), 7.26 (dd, 2H, *J* = 6.8 Hz, 5.0 Hz). M/z (FAB $(M + H)^+$) for $C_8H_6S_2$ 167.26 .

Benzo[1,2-b:4,3-b']dithiophene-4,5-dione (75)[27]

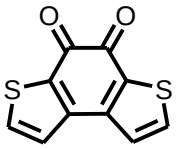

75

Compound **74** (2.0 g, 11.91 mmol) was dissolved in 1,2-dichloroethane (30 mL) . Oxalyl chloride (0.5 mL, 6.18 mmol) was added to the solution. The first portion of the oxalyl chloride was added and the solution was left under reflux for 5 days at 100-110^{o}C. The second portion of the oxalyl chloride was added and the solution was left under reflux for an additional 5 days. The reaction was cooled to room temperature and left overnight to precipitate. A red crude solid was collected by filtration and washed with petroleum ether and warm ethanol and then dried under vacuum to obtain compound **75** (2.1 g , 80%) as a red solid. mp. 261-263^{o}C. ^{1}H NMR (400 MHz, $CDCl_3$) δ = 7.86 (d, 2H, *J* = 5 Hz), 7.32 (d , 2H , *J* = 5 Hz). ^{13}C NMR ($CDCl_3$, 100 MHz) δ 173.8 (C=O), 142.4 (C=C), 138.5 (CH), 135.1 (C=C), 124.8 (CH). M/z (FAB $(M + H)^+$) for $C_{10}H_4O_2S_2$ 221.27.

5- Nitro-1,10-phenanthroline (77)[74]

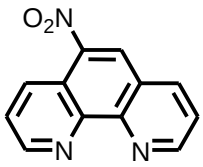

77

Compound **76** (5.0 g, 22.78 mmol) and sulphuric acid (30 mL) was heated under reflux to 160^{o}C. To this fuming nitric acid (15 mL) was added dropwise over 30 min. The solution mixture was left under reflux for 3h. After that the mixture was poured into ice water and adjusted to pH = 3 by adding saturated NaOH. A yellow solid precipitate was collected by filtration and washed thoroughly with water then dried under vacuum to yield **77** (4.0 g, 64 %) as a yellow solid. mp. 215-217^{o}C. ^{1}H NMR (400 MHz $CDCI_3$) δ = 9.41 (dd, 1H, *J* = 4.3 Hz, 1.7 Hz), 9.35 (dd, 1H, *J* = 4.3 Hz, 1.7 Hz), 9.08 (dd, 1H, *J* = 8.6 Hz, 1.7 Hz), 8.75 (s, 1H), 8.48 (dd, 1H, *J* = 8.5 Hz, 1.7 Hz), 7.87 (dd, 1H, *J* = 8.6 Hz, 4.3 Hz), 7.83 (dd, 1H, *J* = 8.6 Hz, 4.3 Hz). ^{13}C NMR ($CDCl_3$, 100 MHz) = 153.7 (CH), 151.9 (CH), 147.8(C), 146.3 (C), 137.9 (C), 132.6 (CH), 125.5 (CH), 125.5 (CH), 124.5 (CH), 124.4 (CH), 121.1 (C). M/z (FAB $(M + H)^+$) for $C_{12}H_7N_3O_2$ 226.0 .

6-Nitro-1,10-phenanthroline-5-amine (78)[101]

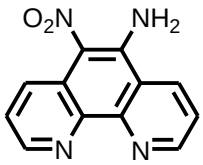

78

To a solution of compound **77** (4.0 g, 17.8 mmol) in methanol (100 mL), hydroxylamine hydrochloride (8.0 g, 115.3 mmol) was added and the solution mixture was heated to reflux. A solution of potassium hydroxide (9.0 g, 160.4 mmol) in methanol (100 mL) was added drop wise over of 45 min then the reaction was heated under reflux for another hour. The reaction was cooled and poured into ice-water (300 mL). The precipitate was filtered and washed with water, methanol, and chloroform then dried under high vacuum to afford **78** (1.43 g, 32 %) as a brown powder. mp. > 300 ^{o}C ^{1}H NMR (400 MHz, DMSO) δ = 9.31 (d, 1H, *J* = 8.6 Hz), 9.01 (dd, 1H, *J* = 8.5 Hz, 1.5 Hz), 8.91 (d, 1H, *J* = 3.5 Hz), 8.48 (d, 1H, *J* = 3.5 Hz), 8.34 (s, 2H, NH_2), 7.59 (dd, 1H, *J* = 8.0 Hz, 4.2 Hz), 7.43 (dd, 1H, *J* = 8.5 Hz, 4.2 Hz). ^{13}C NMR (DMSO, 100 MHz) δ = 206.6, 151.6 (CH), 148.2 (C), 144.3 (CH), 141.1 (C), 133.8 (CH), 131.2 (CH), 128.1 (C), 127.6 (C), 123.4 (CH), 123.3 (CH), 117.6 (C), 79.2 (C-NO_2). M/z (FAB $(M + H)^+$) for $C_{12}H_8N_4O_2$ 241.2.

1,10-Phenanthroline-5,6-diamine (79) [101]

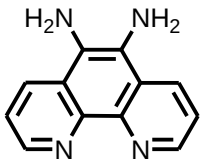

79

Compound **78** (0.2 g, 0.80 mmol), and palladium on carbon (0.1g, 10%) were added to methanol (200 mL). Hydrazine hydride 55% (1.0 mL) was then added to the reaction mixture drop wise over 15 min. The reaction mixture was heated under reflux for a further 45 min and filtered while hot. The solution was concentrated under vacuum and the yellow product was precipitated by the addition of petroleum ether. The mixture was then filtered and washed thoroughly with petroleum ether and dried under vacuum to yield **79** (0.1 g, 59 %) as yellow solid. mp. 160-165^{o}C. ^{1}H NMR (400 MHz DMSO) δ = 8.77 (dd, 2H, J = 4.2 Hz, 1.6 Hz), 8.48 (dd, 2H, J = 8.5 Hz, 1.6 Hz), 7.60 (q, 2H, 4.2 Hz), 5.20 (s, 4H, NH_2). M/z (FAB $(M + H)^+$) for $C_{12}H_{10}N_4$ 211.23.

Dipyrido[2,3-*a*:3',2'-*c*] dithieno[2,3-*h*:3',2'-*j*] phenazine (80)

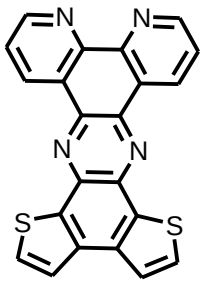

80

A solution of **79** (0.1 g, 0.45 mmol) and compound **75** (0.1 g, 0.45 mmol) in methanol (30 mL) was heated under reflux for 1.5 h. The suspension was filtered while hot. A pale yellow powder was collected and was washed with methanol and diethyl ether to afford **80** (0.12 g, 67 %) as a dark green solid mp. > 300 ^{o}C. ^{1}H NMR (400 MHz, $CDCl_3$) δ = 10.22 (dd, 2H, *J* = 6.4 Hz, 0.8 Hz), 9.42 (dd, 2H, *J* = 5.2 Hz, 0.8 Hz), 8.48 (dd, 2H, *J* = 6.4 Hz, 4.0 Hz), 8.03 (d, 2H, *J* = 4.0 Hz), 7.78 (d, 2H, *J* = 4.0 Hz).^{13}C NMR ($CDCl_3$, 100 MHz) δ = 139.7 (C), 139.2 (CH), 138.3 (C), 138.1 (C), 136.0 (C), 134.6 (C), 133.0 (CH), 130.0 (CH), 129.5 (C), 126.8 (CH), 123.3 (CH). ν_{max} /cm^{-1} 3043*w* (C-H), 1525*s* (C=N), 1492*s* (C=C), 1467*s* (C=C), 1431*s*, 1419*s*, 1361*s*, 1286*m*, 1274*s*, 1226*s*, 1126*s*, 1080*s*, 962*s*, 848*m*. M/z (FAB $(M + H)^+$) for $C_{22}H_{10}N_4S_2$ 395.0420. Anal. Calc. for $C_{22}H_{10}N_4S_2$ (C) 66.98, (H) 2.56, (N) 14.20; found (C) 66.47, (H) 2.43, (N) 13.84.

Dithieno [5,6:7,8]quinoxalino[2,3-*f*]pyrazino[1,2,3,4-*lmn*][1,10] phenanthrolinium, 5,6-dihydro-, hexafluorophosphate(1-) (1:2) (70)

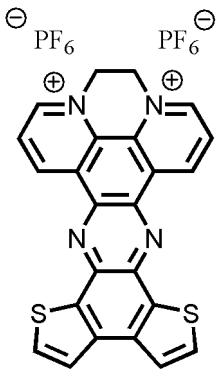

70

A solution of **80** (0.10 g, 0.25 mmol) and 1,2-dibromoethane (7 mL, 81.1 mmol) was heated to 115^{o}C and left overnight. The reaction mixture was cooled to room temperature and precipitated into petroleum ether (50 mL). The precipitate was filtered and washed carefully with chloroform. The precipitate was dissolved in DMF and a dark green precipitate formed upon addition of excess potassium hexafluorophosphate (dissolved in DMF). The mixture was added drop wise to water (50 mL). The resultant product was collected by filtration and washed thoroughly with water to afford **70** (0.04 g, 22 %) as a green solid, mp. > 300 ^{o}C ; ^{1}H NMR (400 MHz, DMSO) δ = 10.50 (dd, 2H, *J* = 8.5 Hz, 1.1 Hz), 9.87 (dd, 2H, *J* = 5.6 Hz, 1.1 Hz), 8.93 (dd, 2H, *J* = 8.5 Hz, 5.6 Hz), 8.54 (d, 2H, *J* = 5.3 Hz), 8.33 (d, 2H, *J* = 5.3 Hz), 5.76 (s, 4H). ^{13}C NMR (DMSO, 100 MHz) δ = 176.9 (C), 149.9 (CH), 143.3 (CH), 141.9 (C), 140.5 (C), 139.3 (C), 135.6 (CH), 131.6 (C), 130.6 (C), 129.6 (CH), 125.1 (CH), 53.1 (CH_2). ν_{max}/cm^{-1} 3041*s* (C-H), 1491*s* (C=C), 1432*s* (C-C), 1417*s*, 1361*s*, 1276*m*, 1121*s*, 1079*s*, 851*s*, 811*m*. M/z (FAB $(M + H)^{+}$)) for $C_{24}H_{14}F_{12}N_4P_2S_2$ is 713.33. Anal. Calc. for $C_{24}H_{14}F_{12}N_4P_2S_2$ (C) 40.46, (H) 1.98, (N) 7.86; found (C) 41.16, (H) 2.04, (N) 7.10.

N-(5-nitro-1,10-phenanthrolin-6-yl)isobutyramide (81)

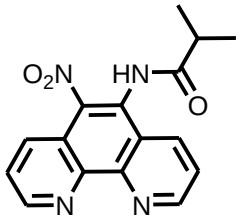

81

To a solution of **78** (0.5 g, 2.1 mmol) in dry DMF (30 mL), isobutyryl chloride (0.3 mL 3.0 mmol) and triethylamine (0.3 g, 3.0 mmol) were added. The reaction mixture was allowed to stir for 24 h. at 80-100 ^{o}C DMF was removed under reduced pressure, and the solution was precipitated into petroleum ether (10 mL) and the yellow precipitate was collected via suction filtration and washed with petroleum ether many times to afford **81** (0.05 g, 10 %) as yellow powder. ^{1}H NMR (400 MHz, $CDCl_3$) **δ =** 9.35 (dd, 1H, *J* = 4.4 Hz, 1.5 Hz), 9.32 (dd, 1H, *J* = 4.4 Hz, 1.5 Hz), 8.38 (dd, 1H, *J* = 8.7 Hz, 1.1 Hz), 8.33 (dd, 1H, *J* = 8.4 Hz, 1.3 Hz), 8.01 (s, 1H, NH), 7.80 (M, 2H), 2.83 (M, 1H, CH_{alph}), 1.42 (d, 6H, *J* = 6.8 Hz). ^{13}C NMR (100 MHz, D_2O): **δ** = 176.9(C), 146.2(C), 144.5(C), 142.5(C), 120.4(C), 118.5(C) ,152.9 (CH); 151.8(CH); 134.4(CH); 131.1(CH); 125.3(CH); 124.9(CH); 19.7(CH_3); 34.7($CH_{alph).}$ ν_{max}/cm^{-1} 3531*w* (N-H), 3352*w* (N-H), 2972*w* (C-H), 1680*m* (C=O amide), 1527*s*(N-O), 1481*s*, 1469*s*, 1425*s*, 1373*s*, 1234*m*, 1228*m*, 1207*m*, 1097*s*, 947*s*, 831*s*, 806*s*, 756*s*, 690*m*. M/z (FAB $(M + Na)^+$) for $C_{16}H_{14}N_4O_3$ is 333.0958. Anal. Calc. for $C_{16}H_{14}N_4O_3$ (C) 61.93, (H) 4.55; (N) 18.06; found (C) 61.04, (H) 4.67, (N) 17.93.

6. Appendix

6.1 ^{1}H NMR spectra of compound 70 and compound 80

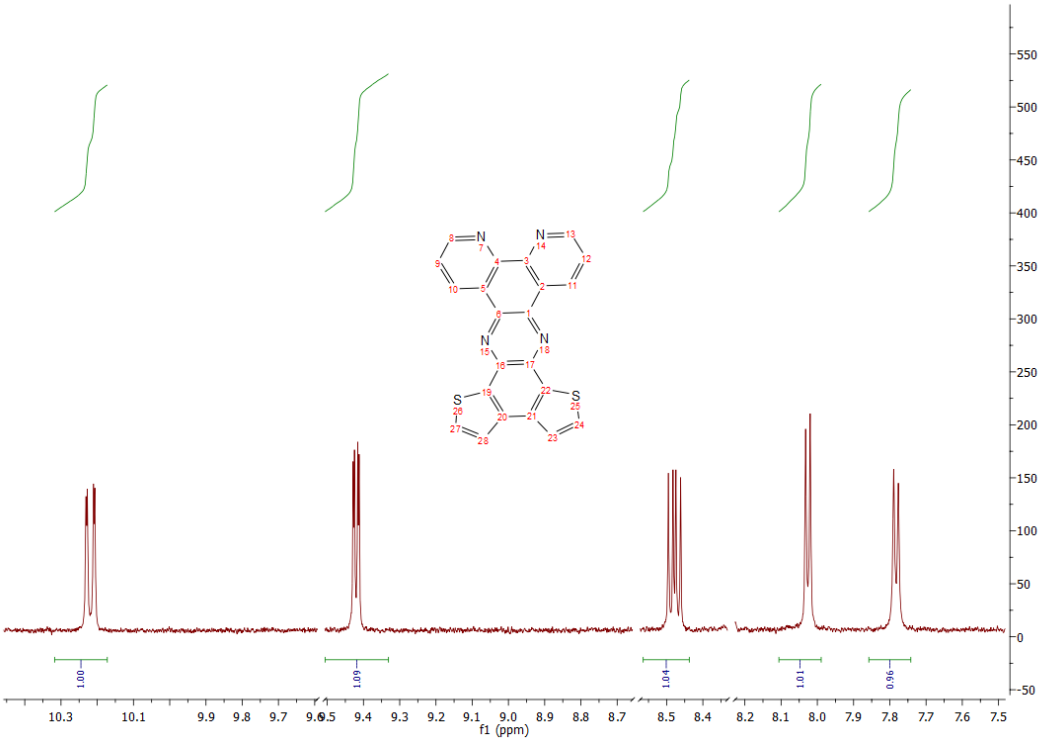

Figure 50. ^{1}H NMR spectra of compound 80.

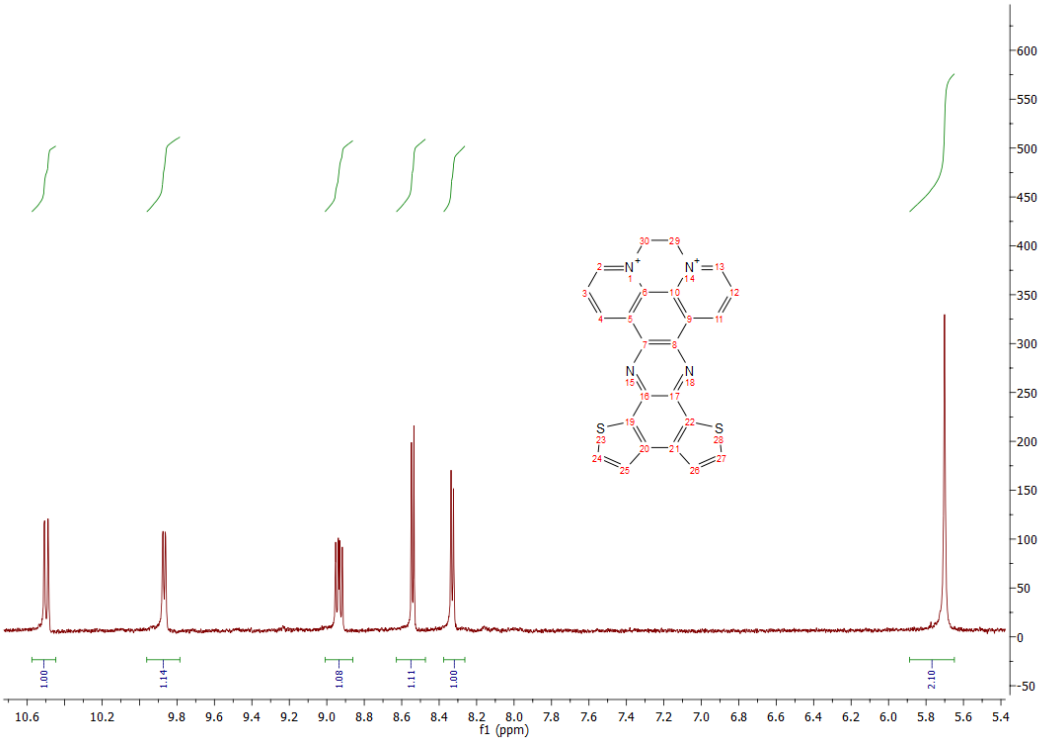

Figure 51. ^{1}H NMR spectra of compound 70.

6.2.1 Cyclic voltametry of polymer of 80

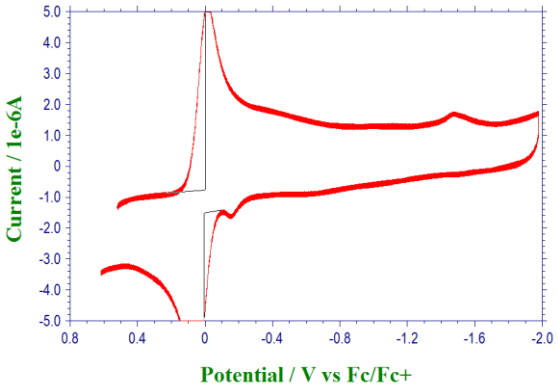

Scan rate 0.15 V/s

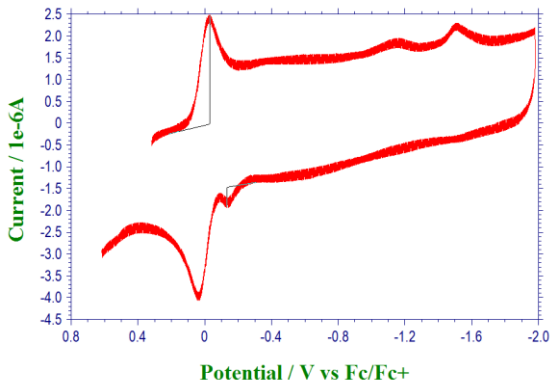

Scan rate 0.20 V/s

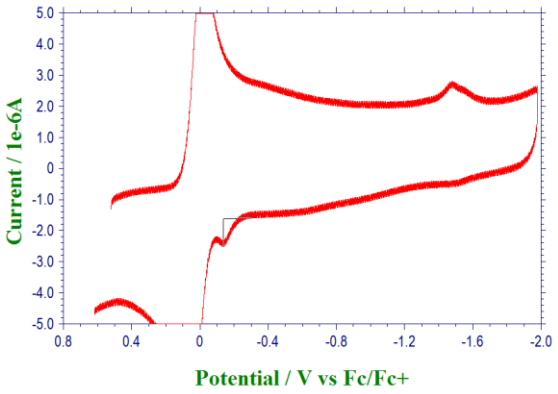

Scan rate 0.25 V/s

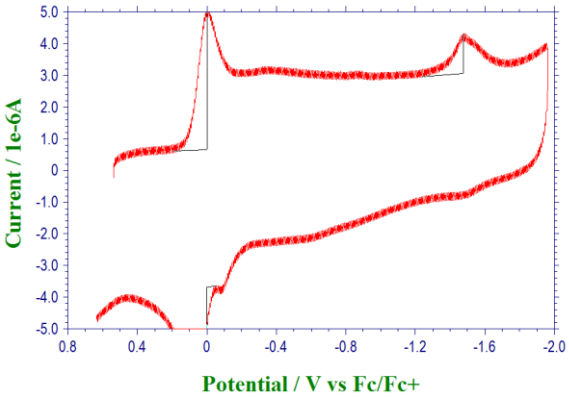

Scan rate 0.40 V/s

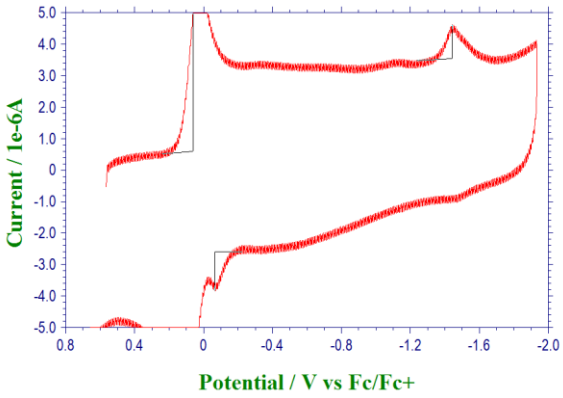

Scan rate 0.45 V/s

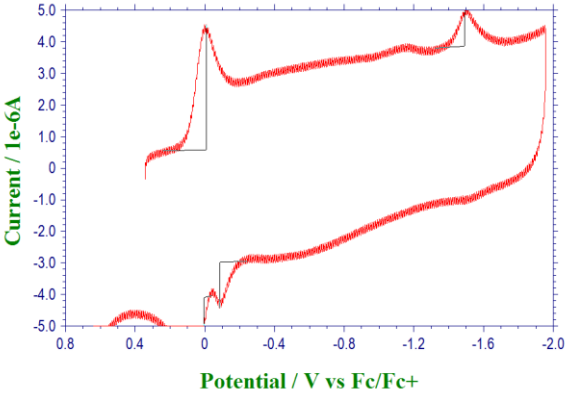

Scan rate 0.50 V/s

6.2.2 Cyclic voltametry of polymer of 70

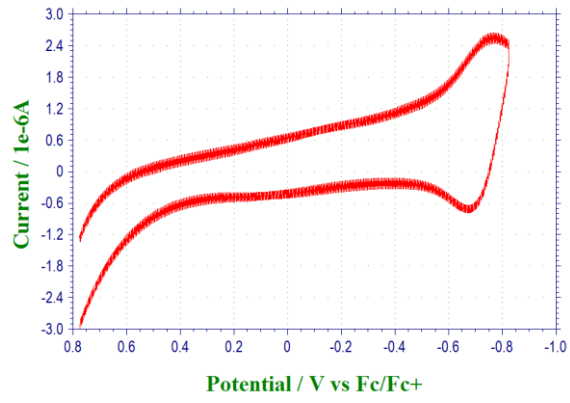

Scan rate 0.2 V/s

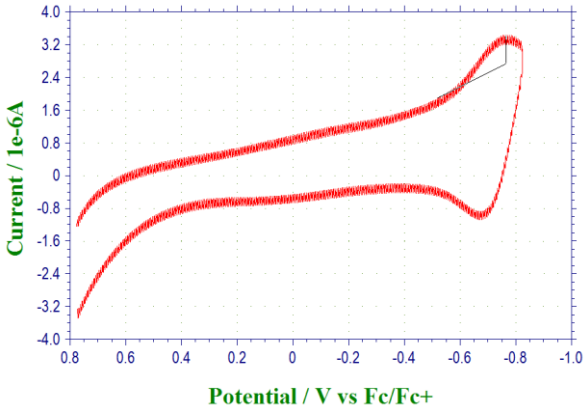

Scan rate 0.3 V/s

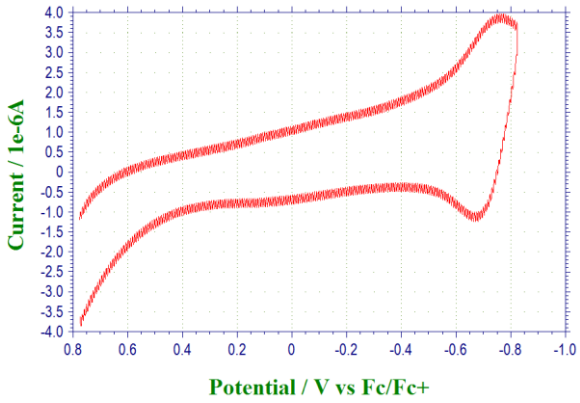

Scan rate 0.4 V/s

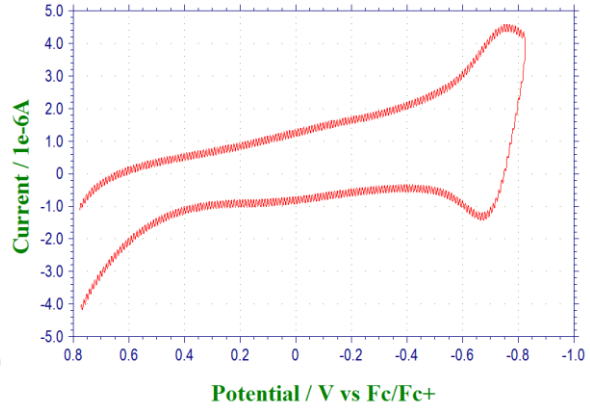

Scan rate 0.5 V/s

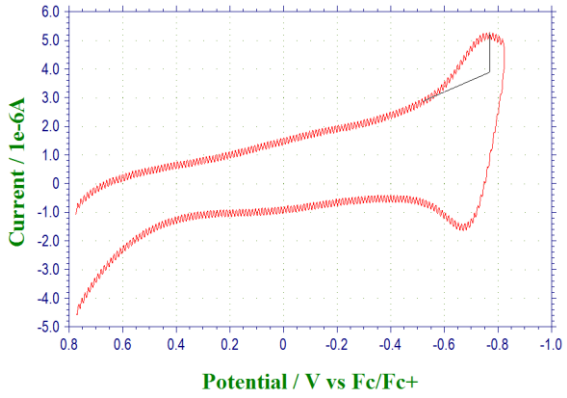

Scan rate 0.6 V/s

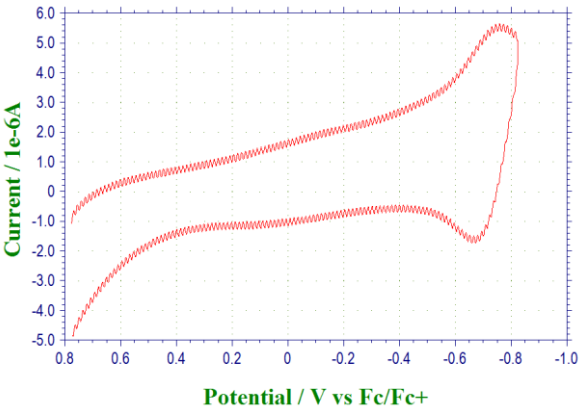

Scan rate 0.7 V/s

References

(1) Carlton, D. M.; McCarthy, D. K.; Genz, R. H., *J. Phys. Chem.*, **1964**, *68*, 2661.

(2) AlSalhi, M. S.; Alam, J.; Dass, L. A.; Raja, M., *Int. j. mol. sci.*, **2011**, *12*, 2036.

(3) Potember, R. S.; Hoffman, R. C.; Hu, H. S.; Cocchiaro, J. E.; Viands, C. A.; Murphy, R. A.; Poehler, T. O., *Polymer*, **1987**, *28*, 574.

(4) Wu, J.-S.; Cheng, S.-W.; Cheng, Y.-J.; Hsu, C.-S., *Chem. Soc. Rev.*, **2015**, *44*, 1113.

(5) Van Mullekom, H. A. M.; Vekemans, J. A. J. M.; Havinga, E. E.; Meijer, E. W., *Mat. Sci. Eng. R.*, **2001**, *32*, 1.

(6) Murahashi, S.; Yamamura, M.; Yanagisawa, K.; Mita, N.; Kondo, K., *J. Org. Chem.*,**1979**, *44*, 2408.

(7) Kosugi, M.; Hagiwara, I.; Migita, T., *Chem. Lett.*, **1983**, *12*, 839.

(8) Scott, W. J.; Stille, J. K. , *J. Am. Chem. Soc.*, **1986**, *108*, 3033.

(9) Jabri, N.; Alexakis, A.; Normant, J. F., *Tetrahedron Lett.*, **1981**, *22*, 959.

(10) Hatanaka, Y.; Hiyama, T., *J. Am. Chem. Soc.*, **1990**, *112*, 7793.

(11) Yamamura, M.; Moritani, I.; Murahashi, S.-I., *J. Org. metal. Chem.*, **1975**, *91*, C39.

(12) Suzuki, A., *J. Org. Metal. Chem.*,**1999**, *576*, 147.

(13) Baba, S.; Negishi, E. , *J. Am. Chem. Soc.*, **1976**, *98*, 6729.

(14) King, A. O.; Negishi, E.; Villani, F. J.; Silveira, A., *J. Org. Chem.*, **1978**, *43*, 358.

(15) Negishi, E.; Takahashi, T.; Baba, S; Van Horn, D. E.; Okukado, N. *J. Am. Chem. Soc.*,**1987**, *109*, 2393.

(16) Stille, J. K., *Angew. Chem. Int. Ed. in English*, **1986**, *25*, 508.

(17) Guram, A. S.; Rennels, R. A.; Buchwald, S. L., *Angew. Chem. Int. Ed. in English*, **1995**, *34*, 1348.

(18) Palucki, M.; Wolfe, J. P.; Buchwald, S. L., *J. Am. Chem. Soc.*, **1996**, *118*, 10333.

(19) Hirao, T.; Masunaga, T.; Ohshiro, Y.; Agawa, T., *Tetrahedron Lett.*, **1980**, *21*, 3595.

(20) Li, G. Y., *Angew. Chem. Int. Ed.*, **2001**, *40*, 1513.

(21) Miyaura, N.; Suzuki, A., *Chem. Rev.*, **1995**, *95*, 2457.

(22) Suzuki, A. *J. Organomet Chem.*, **2002**, *653*, 83..

(23) Cosnier S.; Karyakin A.; *Electropolymerization*; Wiley-VCH Verlag GmbH & Co. KGaA, **2010**.

(24) Beaujuge, P. M.; Reynolds, J. R. ,*Chem. Rev.*, **2010**, *110*, 268.

(25) Popere, B. C.; Della Pelle, A. M.; Thayumanavan, S., *Macromolecules* **2011**, *44*, 4767.

(26) Czichy, M.; Wagner, P.; Grządziel, L.; Krzywiecki, M.; Szwajca, A.; Łapkowski, M.; Żak, J.; Officer, D. L., *Electrochimica Acta* **2014**, *141*, 51.

(27) Meyer, A.; Sigmund, E.; Luppertz, F.; Schnakenburg, G.; Gadaczek, I.; Bredow, T.; Jester, S.-S.; Höger, S. ,*Beilstein, J. Org. Chem.*,**2010**, *6*, 1180.

(28) Arroyave, F. A.; Richard, C. A.; Reynolds, J. R., *Org. Lett.*, **2012**, *14*, 6138.

(29) Xie, Y.; Fujimoto, T.; Dalgleish, S.; Shuku, Y.; Matsushita, M. M.; Awaga, K. ,*J. Mater. Chem., C* **2013**, *1*, 3467.

(30) Mondal, R.; Becerril, H. A.; Verploegen, E.; Kim, D.; Norton, J. E.; Ko, S.; Miyaki, N.; Lee, S.; Toney, M. F.; Bredas, J.-L.; McGehee, M. D.; Bao, Z., *J. Mater. Chem.*,**2010**, *20*, 5823.

(31) (a) Liang, Y.; Xu, Z.; Xia, J.; Tsai, S.-T.; Wu, Y.; Li, G.; Ray, C.; Yu, L., *Adv. Mater.*, 2010, 22, E135. (b) Liu, Y.; Zhao, J.; Li, Z.; Mu, C.; Ma, W.; Hu, H.; Jiang, K.; Lin, H.; Ade, H.; Yan, H., *Nat Commun*, 2014, 5. (c) He, Z.; Xiao, B.; Liu, F.; Wu, H.; Yang, Y.; Xiao, S.; Wang, C.; Russell, T. P.; Cao, Y., *Nat. Photon.*, 2015, 9, 174. (d) You, J.; Dou, L.; Yoshimura, K.; Kato, T.; Ohya, K.; Moriarty, T.; Emery, K.; Chen, C.-C.; Gao, J.; Li, G.; Yang, Y., *Nat Commun.*, 2013, 4, 1446. (e) Li, N.; Baran, D.; Spyropoulos, G. D.; Zhang, H.; Berny, S.; Turbiez, M.; Ameri, T.; Krebs, F. C.; Brabec, C. J., *Adv. Energy Mater.*, 2014, 4, n/a.

(32) (a) Brisset, H.; Navarro, A.-E.; Moustrou, C.; Perepichka, I. F.; Roncali, J., *Electrochem. Commun.*, **2004**, *6*, 249(b) Yuen, J. D.; Fan, J.; Seifter, J.; Lim, B.; Hufschmid, R.; Heeger, A. J.; Wudl, F. , *J. Am. Chem. Soc.*, **2011**, *133*, 20799.

(33) Steckler, T. T.; Henriksson, P.; Mollinger, S.; Lundin, A.; Salleo, A.; Andersson, M. R., *J. Am. Chem. Soc.*, **2014**, *136*, 1190.

(34) Zhang, Q. T.; Tour, J. M., *J. Am. Chem. Soc.*, **1998**, *120*, 5355.

(35) Wamhoff, H., *Angew. Chem.*, **1983**, *95*, 648.

(36) Yamamoto, T.; Zhou, Z.-h.; Kanbara, T.; Shimura, M.; Kizu, K.; Maruyama, T.; Nakamura, Y.; Fukuda, T.; Lee, B.-L.; Ooba, N.; Tomaru, S.; Kurihara, T.; Kaino, T.; Kubota, K.; Sasaki, S., *J. Am. Chem. Soc.*, **1996**, *118*, 10389.

(37) Dennler, G.; Scharber, M. C.; Brabec, C. J,. *Adv. Mater.*, **2009**, *21*, 1323.

(38) Grätzel, M., *J. Photochem. Photobiol. C: Photochem. Rev.*,**2003**, *4*, 145.

(39) Tributsch, H., *Coordination Chem. Rev.*, **2004**, *248*, 1511.

(40) O'Regan, B.; Gratzel, M. *Nature* **1991**, *353*, 737.

(41) Berenede, J. C., *J.Chilean Chem. Soc.,* **2008**, *53*, 1549.

(42) Yum, J.-H.; Baranoff, E.; Wenger, S.; Nazeeruddin, M. K.; Gratzel, M. *Energy & Environmental Science* **2011**, *4*, 842.

(43) Hamann, T. W.; Jensen, R. A.; Martinson, A. B. F.; Van Ryswyk, H.; Hupp, J. T. *Energy & Environmental Science* **2008**, *1*, 66.

(44) Yella, A.; Lee, H.-W.; Tsao, H. N.; Yi, C.; Chandiran, A. K.; Nazeeruddin, M. K.; Diau, E. W.-G.; Yeh, C.-Y.; Zakeeruddin, S. M.; Grätzel, M. *Science* **2011**, *334*, 629.

(45) Monk, P. M. S.; Hodgkinson, N. M. *Electrochimica Acta* **1998**, *43*, 245.

(46) Porter, W. W.; Vaid, T. P.; Rheingold, A. L., *J. Am. Chem. Soc.,* **2005**, *127*, 16559.

(47) Takahashi, K.; Nihira, T.; Akiyama, K.; Ikegami, Y.; Fukuyo, E., *J.Chem. Soc., Chem. Commun.,* **1992**, 620.

(48) Kelley, C. J.; Ansu, K.; Budisusetyo, W.; Ghiorghis, A.; Qin, Y.; Kauffman, J. M., *J. Heterocyclic Chem.,* **2001**, *38*, 11.

(49) Valášek, M.; Pecka, J.; Jindřich; Calleja, G.; Craig, P. R.; Michl, J., *J. Org. Chem.*, **2004**, *70*, 405.

(50) Nakajima, R.; Iida, H.; Hara, T. *B. Chem. Soc. Jpn.,* **1990**, *63*, 636.

(51) Albers, W. M.; Canters, G. W.; Reedijk, J., *Tetrahedron*, **1995**, *51*, 3895.

(52) Happ, J. W.; Ferguson, J. A.; Whitten, D. G., *J. Org. Chem.,***1972**, *37*, 1485.

(53) Yasui, S.; Itoh, K.; Ohno, A.; Tokitoh, N., *Org. Biomol. Chem.,* **2006**, *4*, 2928.

(54) Merz, A.; Reitmeier, S., *Adv. Mater.*, **1989**, *1*, 193.

(55) Zakirov, M. I.; Shandryuk, G. A.; Bondarenko, G. N.; Nodova, E. L.; Kryl'skii, D. V.; Talroze, R. V., *Polym. Sci. Ser., B* **2012**, *54*, 50.

(56) (a) Daube, K. A.; Harrison, D. J.; Mallouk, T. E.; Ricco, A. J.; Chao, S.; Wrighton, M. S.; Hendrickson, W. A.; Drube, A. J., *J. Photochem.,***1985**, *29*, 71(b) Sassoon, R. E.; Gershuni, S.; Rabani, J., *J. Phys. Chem.,***1985**, *89*, 1937(c) Moutet, J.-C.; Pickett, C. J., *J.Chem. Soc., Chem. Commun.,* **1989**, 188.

(57) Shu, C. F.; Wrighton, M. S., *J. Phys. Chem.*, **1988**, *92*, 5221.

(58) Reinhoudt, D. N.; Sudhölter, E. J., *Adv. Mater.,* **1990**, *2*, 23.

(59) Bange, K.; Gambke, T, *Adv. Mater.,* **1990**, *2*, 10.

(60) Bäuerle, P.; Gaudl, K. U., *Synth. Metals,* **1991**, *43*, 3037.

(61) Bäuerle, P.; Gaudl, K. U., *Adv. Mater.,* **1990**, *2*, 185.

(62) Bidan, G.; Deronzier, A.; Moutet, J.-C., *J.Chem. Soc., Chem. Commun.*, **1984**, 1185.

(63) Ko, H. C.; Park, S. A.; Paik, W. K.; Lee, H., *Synth. Metal,s* **2002**, *132*, 15.

(64) Smith, D. K.; Lane, G. A.; Wrighton, M. S., *J. Phys. Chem.*, **1988**, *92*, 2616.

(65) Sariciftci, N. S.; Mehring, M.; Gaudl, K. U.; Bäuerle, P.; Neugebauer, H.; Neckel, A., *J. Phys. Chem.*, **1992**, *96*, 7164.

(66) Yan, X.; Li, Z.; Wei, P.; Huang, F., *Org. Lett.*, **2013**, *15*, 534.

(67) Izuhara, D.; Swager, T. M., *J. Am. Chem. Soc.*, **2009**, *131*, 17724.

(68) Liao, J. H.; Swager, T. M., *Langmuir*, **2007**, *23*, 112.

(69) Suzuka, M.; Hara, S.; Sekiguchi, T.; Oyaizu, K.; Nishide, H., *Polymer*.

(70) Anandan, S., *Current App. Phys.*,**2008**, *8*, 99.

(71) Santa-Nokki, H.; Kallioinen, J.; Korppi-Tommola, J., *Photochem. Photobio. Sci.*, **2007**, *6*, 63.

(72) Guo, L.; Deng, J.; Zhang, L.; Xiu, Q.; Wen, G.; Zhong, C., *Dyes and Pigments*, **2012**, *92*, 1062.

(73) Li, H.-H.; Wu, J.-X.; Dong, H.-J.; Wu, Y.-L.; Chen, Z.-R., *J. Molecular Structure*, **2011**, *987*, 180.

(74) Ji, S.; Guo, H.; Yuan, X.; Li, X.; Ding, H.; Gao, P.; Zhao, C.; Wu, W.; Wu, W.; Zhao, J., *Org. Lett.*, **2010**, *12*, 2876.

(75) Yu, Q.-Y.; Huang, J.-F.; Shen, Y.; Xiao, L.-M.; Liu, J.-M.; Kuang, D.-B.; Su, C.-Y. *RSC Adv.*,**2013.**, *3*, 19311.

(76) Reynal, A.; Forneli, A.; Martinez-Ferrero, E.; Sanchez-Diaz, A.; Vidal-Ferran, A.; Palomares, E., *Eur. J. Inorg. Chem.*,**2008**, *2008*, 1955.

(77) Erten-Ela, S.; Gokhan Colak, S.; Ocakoglu, K., *Inorg. Chimica Acta* **2013**, *405*, 252.

(78) Sikorski, M.; Prukała, D.; Insińska-Rak, M.; Khmelinskii, I.; Worrall, D. R.; Williams, S. L.; Hernando, J.; Bourdelande, J. L.; Koput, J.; Sikorska, E., *J. Photochem. Photobiol. A: Chem.*, **2008**, *200*, 148.

(79) Sikorska, E.; Szymusiak, H.; Khmelinskii, I. V.; Koziołowa, A.; Spanget-Larsen, J.; Sikorski, M., *J. Photochem. Photobiol. A: Chem.*, **2003**, *158*, 45.

(80) (a) Kozioł, J., *Photochem. Photobiol.*, **1969**, *9*, 45 (b) Kasha, M., *J. Chem. Soc., Faraday Transactions 2: Molecular and Chem. Phys.*, **1986**, *82*, 2379(c) Szafran, M. M.; Koziot, J.; Heelis, P. F., *Photochem. Photobiol.*, **1990**, *52*, 353.

(81) Grodowski, M. S.; Veyret, B.; Weiss, K., *Photochem. Photobio.*, **1977**, *26*, 341.

(82) (a) Schöllnhammer, G.; Hemmerich, P., *Europ. J. Biochem.*, **1974**, *44*, 561(b) Knowles, A.; Roe, E., *Photochem. photobiol.*, **1968**, *7*, 421(c) Vaish, S. P.; Tollin, G., *J. bioenergetics*, **1971**, *2*, 61(d) Holmström, B.; Oster, G., *J. Am. Chem. Soc.*, **1961**, *83*, 1867.

(83) Sun, M.; Moore, T. A.; Song, P.-S., *J. Am. Chem. Soc.*, **1972**, *94*, 1730.

(84) Sikorska, E.; Kaziołowa, A., *J. Photochem. Photobiol., A: Chem.*, **1996**, *95*, 215.

(85) Sikorska, E.; Khmelinskii, I. V.; Kubicki, M.; Prukała, W.; Nowacka, G.; Siemiarczuk, A.; Koput, J.; Ferreira, L. F. V.; Sikorski, M., *J. Phys. Chem., A* **2005**, *109*, 1785.

(86) Lorente, C.; Thomas, A. H., *Acc. Chem. Res.*, **2006**, *39*, 395.

(87) Inui, Y.; Shiro, M.; Kusukawa, T.; Fukuzumi, S.; Kojima, T., *Dalton Transactions*, **2013**, *42*, 2773.

(88) Legrand, Y.-M.; Gray, M.; Cooke, G.; Rotello, V. M., *J. Am. Chem. Soc.*, **2003**, *125*, 15789.

(89) Heelis, P. F., *Chem. Soc. Rev.*, **1982**, *11*, 15.

(90) Walsh, C., *Acc. Chem. Res.*, **1980**, *13*, 148.

(91) Miura, R., *Chem. Rec.*, **2001**, *1*, 183.

(92) Müller, F., *Free Radic. Biol.Med.*, **1987**, *3*, 215.

(93) Zen, Y. H.; Wang, C. M., *J. Chem. Soc., Chem. Commun.*, **1994**, 2625.

(94) Pauszek, R. F.; Kodali, G.; Caldwell, S. T.; Fitzpatrick, B.; Zainalabdeen, N. Y.; Cooke, G.; Rotello, V. M.; Stanley, R. J., *J. Phys. Chem., B* **2013**, *117*, 15684.

(95) Yu, X.; Eymur, S.; Singh, V.; Yang, B.; Tonga, M.; Bheemaraju, A.; Cooke, G.; Subramani, C.; Venkataraman, D.; Stanley, R. J.; Rotello, V. M., *Phys. Chem. Chem. Phys.*, **2012**, *14*, 6749.

(96) Campbell, W. M.; Jolley, K. W.; Wagner, P.; Wagner, K.; Walsh, P. J.; Gordon, K. C.; Schmidt-Mende, L.; Nazeeruddin, M. K.; Wang, Q.; Grätzel, M., *J. Phys. Chem., C* **2007**, *111*, 11760.

(97) Takeda, J.; Ota, S.; Hirobe, M , *J. Am. Chem. Soc.*, **1987**, *109*, 7677.

(98) Zainalabdeen, N.; Fitzpatrick, B.; Kareem, M. M.; Nandwana, V.; Cooke, G.; Rotello, V. M., *Int. J. Mol. Sci.*, **2014**, *15*, 4255.

(99) Kobayashi, A.; Ohbayashi, K.; Aoki, R.; Chang, H.-C.; Kato, M., *Dalton Trans*, **2011**, *40*, 3484.

(100) Shirdel, J.; Penzkofer, A.; Procházka, R.; Shen, Z.; Strauss, J.; Daub, J., *Chem. Phy.*, **2007**, *331*, 427.

(101) Bolger, J.; Gourdon, A.; Ishow, E.; Launay, J.-P., *Inorg. Chem.,* **1996**, *35*, 2937.

(102) Vyas, R. N.; Wang, B., *Int. J. Mol. Sci.* ,**2010**, *11*, 1956.